Original Research Paper

Volume - 7 | Issue - 7 | July - 2017 | ISSN - 2249-555X | IF : 4.894 | IC Value : 79.96

Chemistry

WHY MORPHINE IS A MOLECULE CHEMICALLY POWERFUL.THEIR COMPARISON WITH COCAINE

Silvia Antonia Brandán

Cátedra de Química General, Instituto de Química Inorgánica, Facultad de Bioquímica. Química y Farmacia, Universidad Nacional de Tucumán, Ayacucho 471, (4000) San Miguel de Tucumán, Tucumán, Argentina.

ABSTRACT The three free base, cationic and hydrochloride structures of morphine alkaloid in gas and aqueous solution phases were theoretically studied by using the B3LYP/6-31G* method and the polarized continuum (PCM) and solvation models in order to analyze their atomic charges, molecular electrostatic potential, bond orders, frontier orbitals and their topological and vibrational properties. The experimental available FT-IR and FT-Raman spectra for the free base and the hydrochloride species were employed together with the corresponding normal internal coordinates to perform the complete vibrational assignments of those three species of morphine by using the scaled quantum mechanical force field (SQMFF) procedure. The high stabilities observed of morphine in relation to cocaine are supported by the natural bond orbital (NBO) and atoms in molecules (AIM) studies. The frontier orbitals studies evidence that the cationic species of morphine is the most reactive in gas phase while the hydrochloride species in aqueous solution. The force fields for the free base, cationic and hydrochloride structures of morphine were computed and the complete vibrational assignments for their expected 114, 117 and 120 vibration normal modes, respectively were here reported for first time together to their force constants. The presence of O--O interactions in cocaine generates high instability in their species justifying their lower stabilities than the corresponding to morphine. Probably, the lower reactivities observed for the free base and hydrochloride morphine species than the cocaine ones could be explained perhaps because cocaine present the higher electrophilic and nucleophilic indexes.

KEYWORDS : Morphine, vibrational spectra, molecular structure, descriptor properties, DFT calculations

INTRODUCTION

Morphine is the principal constituent of alkaloid opium and since it was synthesized for first time in the 1952 year [1,2] until today, it and their opiate derivatives [3-6] are broadly studied due to their known medicinal use for the treatment of severe pain [7]. Probably, the presence in morphine of five fused cyclical structures constituted by one five members and four of six members rings with a tertiary nitrogen atom confers to it their wide variety of effects ranging from sedation to constipation, as mentioned by Busse [7]. In the tropane alkaloids the pharmacological and medicinal properties are attributed to the bicyclic structure constituted by two fused piperidine and pyrrolidine rings and to the tertiary nitrogen atom belonging to the >N-CH_3 group, as was reported in the literature [8-19]. Perhaps, the presence of five fused rings in morphine different from the only two ones presents in cocaine alkaloid could be the cause that morphine acts most powerfully than cocaine. Therefore, those three free base, cationic and hydrochloride structures found for all tropane alkaloids are also expected for morphine. The crystal and molecular structure of morphine hydrochloride trihydrate [20], hydrochloride anhydrate [21] and a stable polymorph form [22] were already reported in the literature. The identifications of these three morphine species by using the vibrational spectroscopy are of great interest taking into account the importance of morphine and the ease and speed of this technique to register the spectra with little amount of substance. Obviously, the studies of those three structures are necessary to perform the complete vibrational analysis of their infrared and Raman spectra. So far, a complete vibrational analysis only for a theoretical optimized structure of the free base with an energy of −939.8574 a.u. was reported by using the 6-311G** basis set [23]. Here, it is necessary to clarify that the structure optimized in that work was different from the most stable structure obtained in this work by using the same basis set (energy value = -939.8644 a.u.) but the corresponding force field was not determined to perform the vibrational assignments of that free base. Hence, that vibrational analysis was reported not with the most stable free base structure. Besides, in other vibrational study for the free base by using DFT calculations and their infrared and Raman spectrum [24] only thirteen frequencies were assigned by using their most stable structure but their corresponding force field was not considered. Hence, so far the most stable structures of those three morphine species even remain without assign. Furthermore, it is very important to know if the >N-CH_3 groups in those three morphine structures present fast *N*-methyl inversion in solution, as reported for the tropane derivatives at room and low temperatures [25]. Certainly, the vibrational analyses by using the corresponding force fields of those three morphine species are not easy to perform due to the presence of five fused rings in their structures. In this context, the aims of this work are clearly: (i) to study the theoretical three structures of morphine in gas and aqueous solution phases by using the hybrid B3LYP method and the 6-31G* basis set [26,27], (ii) to compute the atomic charges, bond orders, molecular electrostatic potentials, stabilization energies, topological properties and frontier orbitals for the three species in the two media, (iii) to perform their complete vibrational analyses by using their experimental available infrared and Raman spectra, their normal internal coordinates and force fields calculated by using the SQMFF methodology [28] with the Molvib program [29] and finally, (iv) to compare their properties calculated in the two media with those reported for tropane alkaloids, as cocaine or tropane [30,31] including their reactivities and descriptors in both media [32-37].

COMPUTATIONAL INFORMATION

The initial free base, cationic and hydrochloride morphine structures were modelled with the *GaussView* program [38] and later, these structures were optimized with the Gaussian 09 program [39] by using the hybrid B3LYP method at 6-31G* level of theory [26,27]. The calculations were also performed by using the 6-311++G** basis set but some results were included due to the lot of quantity of obtained data. Here, the dimeric species of the hydrochloride form was also considered in this study in accordance with that experimental structure determined by Gelbrich et al. for hydrochloride anhydrate [21]. The simplified structures for the three species of morphine and the identifications of their rings can be seen in **Figure 1** while in **Figures 2** and **3** are shown the theoretical structures and the atoms numbering for those three species and for the dimer of hydrochloride form, respectively.

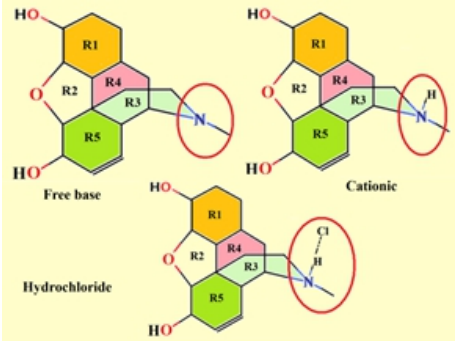

Figure 1. Molecular theoretical structures of the free base, cationic and hydrochloride species of morphine and the numbering and identification of their rings.

Figure 1 shows clearly that the >N-CH3 groups belong to the R3 rings of the three structures while the R2 belong to the furane rings.
These structures were optimized in aqueous solution by using the self-

consistent reaction field (SCRF) method with the integral equation formalism variant polarised continuum (IEFPCM) model [40,41] while the solvation energies of the three species were determined with the solvation model [42] by using the Gaussian program [39].

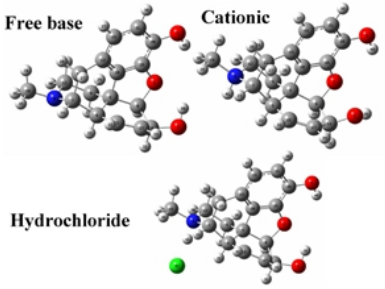

Figure 2. Molecular theoretical structures of the free base, cationic and hydrochloride species of morphine and atoms numbering

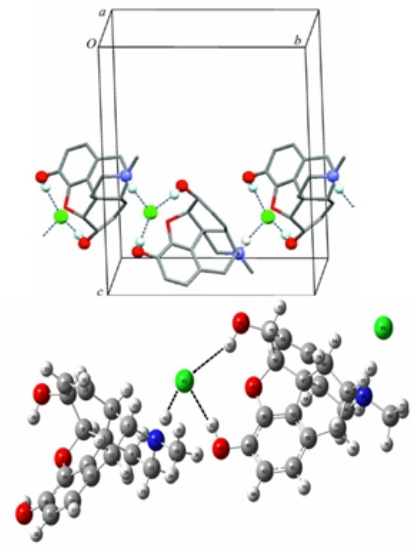

Figure 3. Experimental H bond of morphine anhydrate [21] showing the H, O and Cl atoms involved in H bonds and O-H···Cl and N-H···Cl interactions are drawn as dotted lines (Top). Theoretical structure of hydrochloride dimer of morphine and the atoms numbering (Bottom).

The volume variations that experiment the species in solution were obtained with the Moldraw program [43] by using the same level of theory. The force fields for those three species were determined with the SQMFF approach [28] by using their corresponding normal internal coordinates and the Molvib program [29]. At this point, the normal internal coordinates for the fused five rings of the three species were built as those reported by Rauhut and Pulay [28] for species containing similar rings where three redundant coordinates were removed from each system. Potential Energy Distributions (PED) 10% were considered to perform the assignments of the observed bands in the infrared and Raman spectra to the vibration normal modes. On the other hand, the natural bond orbital (NBO) program [44] was used to study the atomic natural population (NPA) charges, bond orders expressed as Wiberg indexes and, the main donor-acceptor interactions while the Merz-Kollman (MK) charges [45] were also computed to obtain the molecular electrostatic potential values for those species at the same level of theory. In addition, the topological properties were also calculated for all species by using the AIM2000 program [46] and taking into account the parameters suggested by Bader [47]. The prediction of reactivities and behaviours of those three morphine species in both media were carried out by using the frontier orbitals [32,33] and recognized descriptors from the literature [34-37].

RESULTS AND DISCUSSION

Structural studies in gas phase and in solution

In **Table 1** it is possible to observe the total energies, dipole moments, volume variations and solvation energies for the free base, cationic and hydrochloride morphine forms compared with the corresponding reported for the three cocaine's species in gas and aqueous solution phases [31]. First, it is observed that the hydrochloride species of morphine present the higher volumes in both media, as in the similar species of cocaine while the cationic species of both alkaloids have the higher dipole moment values, as can be seen in **Figure S1**. These graphics show that the vectors of the dipole moments for the three species of morphine exhibit different orientations and directions. Similar behaviours in the dipole moments and in volume values for morphine and cocaine are observed in **Figure S2**.

TABLE – 1

Calculated total energies (*E*), dipole moments (μ), volume variations (V) and solvation energies (G) for the free base, cationic and hydrochloride morphine forms compared with those reported for the cocaine's species in gas and aqueous solution phases.

B3LYP/6-31G*				
Gas phase				
Species	E (Hartrees)	μ (D)	V (Å^3)	
Free base	-939.6185	2.77	292.7	
Cation	-939.9999	11.71	295.8	
H-Cl	-1400.4406	7.82	318.3	
PCM				
	E (Hartrees)	μ (D)	V (Å^3)	V (Å^3)
Free base	-939.6367	4.86	293.0	0.3
Cation	-940.1075	18.34	295.0	-0.8
H-Cl	-1400.4859	11.63	319.0	0.7
Solvation energy (kJ/mol)				
	Gu#	Gne	Gc	
Free base	-47.74	13.17	-60.91	
Cation	-282.23	26.96	-309.19	
H-Cl	-118.82	25.92	-144.74	
Cocaine				
Gas phase				
Species	E (Hartrees)	μ (D)	V (Å^3)	
Free base	-1016.1192	1.55	321.0	
Cation	-1016.5254	9.57	322.5	
H-Cl	-1476.9360	7.45	353.2	
PCM				
	E (Hartrees)	μ (D)	V (Å^3)	V (Å^3)
Free base	-1016.1351	1.86	322.2	1.2
Cation	-1016.6092	13.22	323.7	1.2
H-Cl	-1476.9758	12.58	352.5	-0.7
Solvation energy (kJ/mol)				
	Gu#	Gne	Gc	
Free base	-41.70	28.51	-70.21	
Cation	-219.81	38.58	-258.39	
H-Cl	-104.39	38.20	-142.59	

$G_u^{\#}$, See text

On the other hand, the volume variations for these species were calculated, with the Moldraw program [43] as the difference between the values in gas phase and those computed in aqueous solution, which reveals volume contraction in the cationic morphine species different from the cocaine species where their hydrochloride form presents volume contraction in solution. This observation for the cationic species of morphine could be probably related to their higher hydration in solution, as supported by their higher dipole moment and solvation energy values. The volume variations and the solvation energies are graphed in **Figure S3** where the free base and cationic species of cocaine show higher values than the corresponding to morphine while the hydrochloride species of morphine present the higher value than the corresponding to cocaine. The solvation energies show the same behavior in the three species of both alkaloids presenting the higher negative values both cationic species.

The calculated geometrical parameters for the free base, cationic and hydrochloride morphine species in gas and aqueous solution phases were compared with the corresponding experimental ones reported for the free base and hydrochloride morphine [20-22] in **Table 2** by using the root-mean-square deviation (RMSD). The comparisons with the observed values show that the bond lengths and angles present a better correlation or low rmsd values for the stable polymorph form [22]. Hence, in **Figure S4** are compared the predicted bonds lengths belonging to the R1 and R2 rings of the three morphine species calculated in gas phase and aqueous solution at the B3LYP/6-31G* level of theory compared with those experimental corresponding to hydrochloride morphine [22].

TABLE – 2

Comparison of calculated geometrical parameters for the free base, cationic and hydrochloride morphine species in gas and aqueous solution phases compared with the corresponding experimental ones for hydrochloride morphine.

Parameters	B3LYP/6-31G*[a]						Exp[b]	Exp[c]
	Free base		Cationic		Hydrochloride			
	Gas	PCM	Gas	PCM	Gas	PCM		
Bond lengths (Å)								
N4-CH_3	1.453	1.460	1.500	1.497	1.483	1.493	1.490	1.492(2)
N4-C7	1.474	1.484	1.551	1.534	1.514	1.526	1.530	1.517(2)
N4-C12	1.463	1.469	1.523	1.511	1.497	1.505	1.510	1.497(2)
C6-C5	1.549	1.549	1.539	1.550	1.549	1.549	1.550	1.538 (2)
C6-C7	1.555	1.553	1.554	1.551	1.553	1.551	1.550	1.575 (2)
C5-C9	1.546	1.544	1.550	1.545	1.546	1.545	1.540	1.543(2)
C9-C12	1.531	1.528	1.526	1.524	1.528	1.525	1.520	1.516 (2)
C5-C10	1.508	1.508	1.507	1.507	1.508	1.508	1.500	1.503 (2)
C7-C11	1.565	1.563	1.544	1.547	1.551	1.548	1.540	1.540 (2)
C10=C13	1.385	1.386	1.383	1.385	1.385	1.385	1.360	1.380 (2)
C11-C13	1.516	1.516	1.516	1.516	1.518	1.516	1.520	1.511 (2)
C10-C16	1.378	1.382	1.379	1.381	1.378	1.381	1.370	1.370 (2)
C5-C8	1.555	1.556	1.552	1.556	1.555	1.553	1.550	1.549 (2)
C8-O1	1.476	1.473	1.460	1.471	1.478	1.477	1.470	1.466 (18)
C16-O1	1.382	1.380	1.383	1.379	1.379	1.383	1.370	1.377 (17)
C8-C14	1.553	1.554	1.578	1.555	1.553	1.553	1.520	1.536 (2)
C15=C17	1.336	1.337	1.333	1.336	1.336	1.336	1.360	1.320 (2)
C14-C17	1.515	1.509	1.508	1.508	1.516	1.513	1.490	1.506 (2)
C14-O2	1.417	1.427	1.414	1.425	1.416	1.426	1.460	1.419 (19)
C20-O3	1.369	1.381	1.356	1.378	1.365	1.378	1.370	1.375 (2)
RMSD[b]	**0.025**	**0.022**	**0.021**	**0.015**	**0.017**	**0.015**		
RMSD[c]	**0.019**	**0.016**	**0.016**	**0.011**	**0.010**	**0.010**		
Bond angles (º)								
C18-N4-C7	114.1	113.0	114.1	114.2	114.5	113.9	111.0	112.9(14)
C18-N4-C12	112.2	110.3	111.7	111.8	111.9	111.5		111.8(13)
C7-N4-C12	113.4	112.0	113.3	112.6	113.4	112.8	114.0	112.69(13)
N4-C12-C9	111.0	111.5	111.0	110.8	110.7	111.2	109.0	111.09(13)
N4-C7-C6	107.0	107.3	106.1	106.3	106.8	106.6		106.60(12)
C7-C6-C5	106.4	106.7	106.8	107.1	106.6	107.0		107.56(12)
C12-C9-C5	112.0	112.1	111.4	112.7	112.1	112.5		112.00(13)
C6-C5-C9	108.4	108.5	108.2	108.9	108.7	108.8	111.0	109.10(12)
C6-C5-C10	106.4	106.2	109.0	106.4	106.8	106.6	112.0	106.19(12)
C5-C10-C13	127.3	126.8	127.9	126.9	127.4	126.9	112.0	126.61(14)
C7-C11-C13	114.3	114.6	114.0	114.4	114.2	114.4		114.53(14)
C10-C13-C11	118.1	118.3	117.4	118.4	118.0	118.5	123.0	118.42(14)
C8-C5-C10	100.6	100.4	98.9	100.5	100.7	100.7	109.0	100.58(12)
C8-O1-C16	106.9	106.9	105.4	107.0	107.1	107.0		106.96(11)
C6-C5-C8	116.6	116.6	118.1	116.4	116.4	116.4	111.0	115.78(12)
C5-C8-C14	114.1	113.0	114.4	113.0	114.1	114.0	111.0	112.69(12)
RMSD[b]	**6.5**	**6.4**	**6.9**	**6.3**	**6.5**	**6.3**		
RMSD[c]	**0.7**	**0.6**	**1.3**	**0.5**	**0.7**	**0.5**		
Dihedral angles (º)								
C9-C12-N4-CH_3	-172.6	-176.6	-176.8	-175.2	-174.1	-176.4		
C6-C7-N4-CH_3	165.3	170.0	171.0	168.4	167.5	169.5		
N4-C7-C6-C5	65.7	66.1	65.7	65.8	65.3	65.8		
N4-C7-C11-C13	-90.8	-92.2	-84.0	-93.1	-90.3	-92.3		
C7-C6-C5-C8	170.9	171.3	164.7	169.6	169.5	169.8		
C7-C6-C5-C10	59.6	60.3	52.8	58.4	57.8	58.3		
C7-C6-C15-C17	-158.5	-159.9	-146.2	-159.2	-157.6	-158.0		
C11-C13-C10-C16	-164.7	-165.0	-168.7	-165.1	-163.9	-164.9		
O1-C16-C20-O3	5.3	5.1	2.7	4.9	5.3	4.9		
O2-C14-C8-O1	-36.0	-34.0	-2.4	-33.5	-35.6	-34.8		
O2-C14-C17=C15	164.4	165.9	138.8	165.5	164.3	163.7		

[a]This work, [b]Ref [20,21] for hydrochloride morphine; [c]Ref [22] for free base morphine.

In the R1 ring, the behaviors in both media are practically the same in the three species where obviously, the low values observed in the C15=C17 bonds are justified because they have in the three species double bond characters. Only a slight difference in the C8-C14 value for the cationic species it was observed in gas phase. In the R2 ring, the lower values in both media are observed in the C10=C16 and C16-O1 bonds while the longer distance are observed in the C5-C8 bonds. At this time, the observations more interesting are observed in the R3 rings of the three species, as can be seen in **Figure S5**, because the behaviors follow the same tendency in the three species but the values are completely different, especially between the N4-C18, N4-C7 and N4-C12 bonds. In solution, the values for these three bonds in the cationic and hydrochloride species are closer to the two experimental values but different from the values for the free base. When the bond angles are analyzed graphically in **Figure S6** for the three morphine species in gas phase and aqueous solution at the B3LYP/6-31G* level of theory compared we observed that in the gas phase the behaviors are similar to the experimental values corresponding to the hydrochloride morphine [22] however in solution the values for all the species are different from the experimental ones. In all species, the C5-C10=C13 angles have the higher values while the C8-C5-C10 angles the lower ones. Note that the C5-C10=C13 angles are common to the R2, R4 and R5 rings.

Charges, molecular electrostatic potential and bond orders (BO) analysis

Two, MK and NPA charges, the molecular electrostatic potential (MEP) and bond orders (BO) were studied for the three morphine species because they explain the distributions of charges on each species, predict the principal reaction sites and, also describe the characteristic of the different bonds in their structures. Thus, the results from **Table S1** (Supporting material) show the MK charges values on all atoms together with the corresponding MEP values derived from these charges for all species in both media while in **Table S2** are presented the atomic natural population (NPA) charges together with the bond order values expressed, as Wiberg indexes. In **Figure S7** it is possible to observe the variations of those MK charges on the O, N and C atoms corresponding to those three morphine species in both media at the B3LYP/6-31G* level of theory. Analyzing the charges on the O atoms, the higher values are observed on the O2 atoms of the three species which diminishing in solution together with the charges on the O1 atoms. On the contrary, the MK charges on the O3 atoms slightly increase in solution. Besides, the charges on the N atoms decrease in solution probably due to the hydration in these regions. In relation to the H atoms, the higher positive values are observed on the H atoms corresponding to the two OH groups of the three species, as expected because these groups are probably the most labile in solution because these present the lower MEP values. Besides, the H atoms corresponding to the N-H groups of the cationic and hydrochloride species have low MEP values and, as a consequence they are also labile. The evaluation of both charges on the C atoms reveals that the C18 atoms present the most negative values possibly because these atoms belong to the CH_3 groups. On the other hand, on the C14 atoms corresponding to the free base and to the hydrochloride species can be seen the higher positive values different from the cationic form whose C8 atoms present the high charges values. Moreover, in the three species these charges values increase in solution, as shown in Table S1. When the MEP values on the different atoms of the three species are analyzed exhaustively from Table S1 any significant differences among them were found but, when the surfaces mapped for these species are graphed in gas phase at the B3LYP/6-31G* level of theory different colorations range are observed on these surfaces. Thus, in **Figure S8** are presented the electrostatic potential surfaces on the molecular surfaces of the free base, cationic and hydrochloride morphine species in gas phase. The red and blue colorations and their ranges are different in the three species. This way, in the free base the red colours are observed on the O2, O3 and N4 atoms while the blue colours on the H39 and H40 atoms. In the hydrochloride species, the blue colours can be also seen on these H atoms but the strong red colours are observed on the Cl atom and on the O2 and O3 atoms. On the contrary, the entire cationic surface presents blue colour, as expected, because it is a positively charged species. Obviously, we observed the increase in both colorations when the mapped surface for the hydrochloride dimer is presented, as observed in **Figure S9**. Hence, the red regions are clearly nucleophilic sites while the blue colour electrophilic ones.

Table S2 show the NPA charges and the bond orders expressed as Wiberg indexes for the three morphine species at the same level of theory while in **Figures S10** and **S11** are represented the variations of both properties for the O, N and C atoms. The NPA charges practically do not change in solution and the higher negative values are observed on the O2, N4, C11 and C18 atoms of the three species while the higher positive values are observed on the H39 and H40 atoms probably because these atoms are the most labile in both media.

In relation to the BO values we observed from Figure S11 that the O1 and C5 atoms of all species present the higher values while the H atoms belong to the OH groups have the most low BO values, as was also evidenced by the MK and MEP studies.

Stability studies by using NBO and AIM calculations

It is very important to investigate the stabilities of the three morphine species in order to understand why morphine is most powerful than cocaine. Hence, the donor-acceptor energy interactions for the three structures of morphine in both media were studied by using the NBO program [44] and hybrid B3LYP/6-31G* level of theory which are summarized in **Table S3** and compared with the values corresponding to cocaine [31]. Analyzing first the morphine species we observed clearly that the hydrochloride species have higher stabilities in both media than the other ones and, including than the same species corresponding to cocaine. The high stabilities of these species can be attributed to the two $\Delta ET_{\sigma\rightarrow LP^*}$ and $\Delta ET_{LP\rightarrow LP^*}$ interactions observed only for these forms in both morphine and cocaine species. Besides, this study shows that both species have each five charge transfers of which one of them is different both in morphine and in cocaine species, thus, in morphine are observed the $\Delta ET_{\sigma\rightarrow LP^*}$, $\Delta ET_{\pi\rightarrow\pi^*}$, $\Delta ET_{\pi^*\rightarrow\pi^*}$, $\Delta ET_{LP\rightarrow\pi^*}$ and $\Delta ET_{LP\rightarrow LP^*}$ delocalizations while in cocaine are observed the $\Delta ET_{\sigma\rightarrow LP^*}$, $\Delta ET_{\pi\rightarrow\pi^*}$, $\Delta ET_{\pi^*\rightarrow\pi^*}$, $\Delta ET_{LP\rightarrow\sigma^*}$ and $\Delta ET_{LP\rightarrow LP^*}$ delocalizations. Hence, in morphine in the two media are only observed the $\Delta ET_{LP\rightarrow\pi^*}$ interactions while in cocaine only the $\Delta ET_{LP\rightarrow\sigma^*}$ interactions. This way, the total energy in both media favours to the three morphine species. The high stabilities of the three morphine species than the cocaine ones are clearly revealed by this study.

The intra-molecular interactions for those three morphine species were also investigate by using the topological properties in accordance with the Bader theory [47] and by using the AIM2000 program [46]. The numbers of interactions are important to predict the stabilities of a species. Thus, in **Table S4** are presented the electron density, $\rho(r)$, the Laplacian values, $\nabla^2\rho(r)$, the eigenvalues $(\lambda 1, \lambda 2, \lambda 3)$ of the Hessian matrix and, the $|\lambda 1|/\lambda 3$ ratio calculated in the bond critical points (BCPs) and in the ring critical points (RCPs) for the free base and cationic species of morphine compared with the corresponding to cocaine. On the other hand, the results for the hydrochloride species are obtained in **Table S5**. Analyzing first the results of Table S4 it is observed only one H bond interaction in the free base of morphine with different characteristic in gas phase than in aqueous solution. Thus, in gas phase it is observed the O1---H39 interaction while in solution it is observed the H28---H34 interaction. The comparisons with the species corresponding to cocaine show that the same O3---H31 interactions are observed in both media. Hence, both free base of morphine and cocaine can be differenced by the number of rings and their properties. The cationic species of morphine do no present interaction in gas phase but in solution it is observed the only H28---H34 interaction while in the cocaine species one interaction is observed in gas phase but in solution two new O---H and C---H interactions are observed. On the other hand, the hydrochloride species of morphine present three new halogen bonds in gas phase but in solution there are reduced to two. A similar result was observed in the corresponding species of cocaine, as can be seen in Table S5. Here, the fundamental difference between morphine and cocaine are evidently the O---O interactions observed only for cocaine in both media. Probably, these interactions generate instability of this hydrochloride cocaine species as compared with the corresponding to morphine especially because the topological properties of the O---O interactions are higher than the Cl---H interactions observed in morphine. This AIM study reveals clearly why the three forms of morphine are different of those corresponding to cocaine.

Frontier orbitals and descriptors evaluation

The above NBO and AIM studies have evidenced notable difference among the three morphine species as compared with cocaine. For these reasons, the frontier orbitals and some descriptors were also

investigate for the three species of morphine in both media in order to predict their reactivities and behaviour in those two media. Hence, in **Table S6** it is summarized the calculated HOMO and LUMO orbitals, energy band gap [33,34], chemical potential (μ), electronegativity (χ), global hardness (η), global softness (S), global electrophilicity index (ω) and global nucleophilicity index (E) [34-37] for the free base, cationic and hydrochloride structures of morphine, cocaine and tropane in gas phase and in aqueous solution by using the hybrid B3LYP/6-31G* level of theory. The comparisons with the cocaine and tropane alkaloids can be seen in **Figures S12** and **S13**. When the gap values are compared for the three alkaloids in both media in Figure S12 we observed that the gap values for tropane in both media have the lowest values and, where clearly their cationic species show the most negative gap values indicating that these species are the less reactive in both media while the hydrochloride species of cocaine in both media are the most reactive because these species present the lower gap values (yellow colours in Fig. S12). On the other hand, the three morphine species show values very closer among them especially in gas phase while the tropane species exhibit different values among them, as observed in Figure S12. For morphine we observed that the cationic species is the most reactive in gas phase while in aqueous solution the hydrochloride species is the most reactive. Hence, the free base is the less reactive species of morphine in both media while in the cocaine and tropane alkaloids the cationic forms are the less reactive and, as a consequence the most stable. The most important results observed in this study are that in aqueous solution, the hydrochloride forms of the three alkaloids are the most reactive being cocaine most reactive than morphine. Probably, the lower reactivities observed for the free base and hydrochloride morphine species than cocaine ones could be explained by the five different rings present in morphine.

Analyzing the descriptors of Table S6 and Figure S13 we observed clearly that the three different cationic species have higher values, where in particular the species corresponding to cocaine present the higher electrophilic and nucleophilic indexes. Probably, these higher values observed in the hydrochloride species of cocaine than morphine explain the higher reactivity observed for these species. Moreover, the different biological activities observed in morphine could be possibly attributed to the formation of some of the three species in solution.

VIBRATIONAL ANALYSIS

The hybrid B3LYP/6-31G* calculations have optimized the free base, cationic and hydrochloride structures of morphine with C_1 symmetries and have predicted for each species 114, 117 and 120 vibration normal modes, respectively. All vibration modes have activities in both infrared and Raman spectra. In **Figures 4** and **5** can be seen the comparisons among the experimental available infrared spectra in the 4000-0 and 500-150 cm^{-1} regions [23,48] and the corresponding predicted by calculations for the three species of morphine.

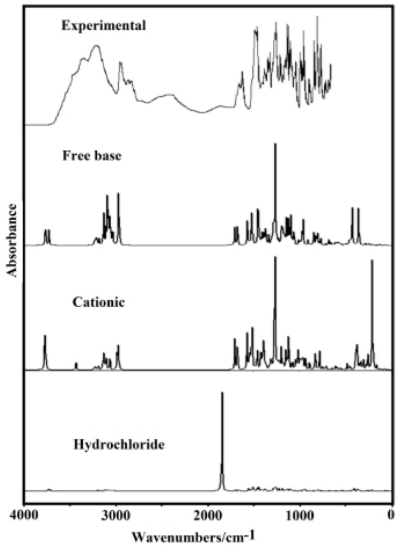

Figure 4. Comparisons between the experimental available FTIR spectra of free base of morphine in the solid state [48] with the corresponding predicted for the free base, cationic and hydrochloride species in the gas phase at B3LYP/6-31G** level of theory.

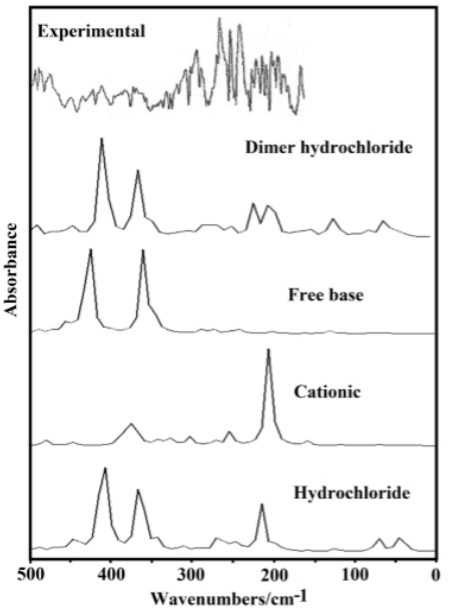

Figure 5. Comparisons between the experimental available FTIR spectra of free base of morphine in the solid state in the 500-150 cm^{-1} region [23] with the corresponding predicted for the free base, cationic and hydrochloride species in the gas phase at B3LYP/6-31G** level of theory.

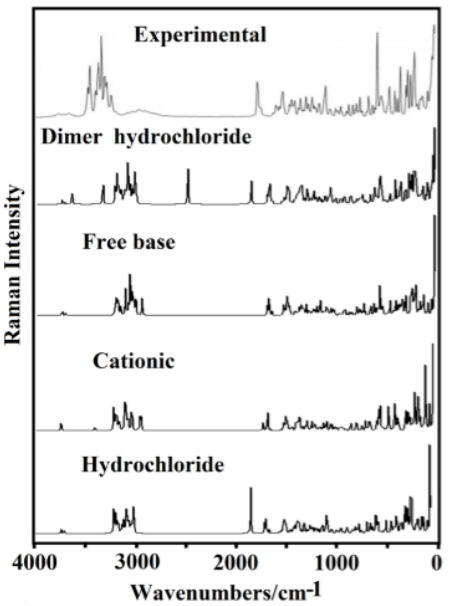

Figure 6. Comparisons between the experimental available Raman spectra of hydrochloride species of morphine in the solid state [24] with the corresponding predicted for the free base, cationic and hydrochloride species in the gas phase at B3LYP/6-31G** level of theory.

When the Raman activities obtained from the calculations are converted in Raman intensities by using recognized equations [49,50] it is possible to observe very good agreement among them. In morphine, as in cocaine probably the hydrochloride species is present as cationic species because the intense IR band predicted for this specie by calculations is not observed very intense in the experimental IR spectrum but as a weak and broad band. The differences observed between both experimental and theoretical spectra are attributed to the calculations (isolated molecules) where the packing forces were not considered. The force fields for the three species of morphine were calculated by using the normal internal coordinates, the SQMFF methodology and scale factors reported for the 6-31G* basis set [28] where the frequencies were scaled with the Molvib program [29].

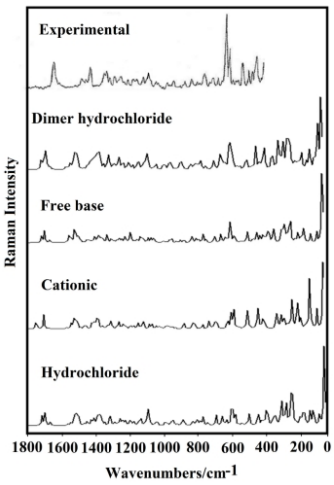

Figure 7. Comparisons between the experimental available Raman spectra of hydrochloride species of morphine in the solid state in the 1800-400 cm^{-1} region [24] with the corresponding predicted for the free base, cationic and hydrochloride species in the gas phase at B3LYP/6-31G** level of theory.

The complete assignments for the three species were performed considering the potential energy distribution (PED) contributions ≥10 % while for the hydrochloride dimer the vibration modes were performed with the aid of the *GaussView* program [38]. The observed and calculated wavenumbers for the three species of morphine with the proposed assignments are presented in **Table 3**. Discussions on the assignments for some important groups are presented below.

Band Assignments

NH modes. These vibration modes only for the cationic and hydrochloride species are expected. Thus, the N-H stretching mode in the cationic tropane alkaloid was assigned at 3419 cm^{-1} while the band at 1626 cm^{-1} was assigned to this mode for the hydrochloride species [30]. These modes in clonidine hydrochloride were assigned to 3427 and 1711 cm^{-1} [51] and in other species containing this groups these modes are assigned between 3480 and 3254 [35,52-54]. For the cationic and hydrochloride species of the cocaine alkaloid these modes were assigned to 2982/2981 and 2545 cm^{-1}. In morphine, the IR bands at 3356, 1855 and 2436 are assigned to these stretching modes corresponding to the cationic, hydrochloride monomer and dimer, respectively, as observed in Table 3. Here, it is necessary to clarify that the N-H stretching mode for the hydrochloride species was predicted at 1776 cm^{-1} with a very high intensity and coupled with the Cl42-H41 stretching mode than the cationic ones. In the cationic and hydrochloride species of tropane the out-of-plane deformation modes were assigned between 1626 and 1393 cm^{-1} [30] while in the cationic species of cocaine are predicted at 1528/1404 cm^{-1} [31] and for hydrochloride at 1490/1365 cm^{-1}. Obviously, in these alkaloids the N atoms have sp^3 hybridizations; hence, the in-plane deformation modes are not observed in the cationic and hydrochloride species. In the two morphine species these modes are predicted at 1428/1417 and 1498/1468 cm^{-1} and, for these reasons, they are assigned in those regions.

CH modes. In the three morphine species, as in the corresponding to cocaine are expected two different C-H groups, one of them aromatics, where the stretching, in-plane and out-of-plane deformation modes are due to the C atoms with sp^2 hybridization and, the other aliphatic ones, the stretching, out-of-plane deformation or rocking modes corresponding to the C atoms with sp^3 hybridization. Evidently, the aromatic C-H stretching modes are assigned at higher wavenumbers because they are predicted by calculations between 3216 and 3034 cm^{-1} while the aliphatic C-H stretching modes are assigned between 2992 and 2828 cm^{-1} for which these modes are assigned in these regions. The in-plane (CH only for aromatics) and out-of-plane deformation modes (CH for aromatics and ρCH for aliphatics) for the three morphine species are assigned between 1511/1149 and 994/808 cm^{-1} but in the hydrochloride dimer these CH modes are predicted from 984 up to 656 cm^{-1}, as indicated in Table 3.

CH_3 modes. In the three morphine species there is only one CH_3 group for which only nine vibration normal modes related to these groups are expected for each species. For the free base, the SQM/B3LYP/6-31G* calculations have predicted one of the antisymmetric modes as a mode pure and with much higher intensity in the Raman spectrum than the corresponding to the cationic and hydrochloride species while in the cationic species those modes are predicted with low intensities in the Raman spectrum. On the other hand, the symmetric modes in the three species are predicted at lower wavenumbers than the corresponding antisymmetric ones. In morphine, both antisymmetric and symmetric modes are assigned to the IR and Raman bands between 3206 and 2865 cm^{-1} because in the three cocaine species these modes were assigned between 3056 and 2845 cm^{-1} [31] while in tropane alkaloid they were assigned between 3098 and 2966 cm^{-1} [30]. Three antisymmetric and symmetric deformation modes for the morphine species are predicted coupled with other modes, with exception of the symmetric mode for the hydrochloride species which is predicted as pure with a contribution PED of 56%. In tropane, these modes are predicted between 1478 and 1400 cm^{-1} [30] while in cocaine between 1474 and 1409 cm^{-1} and, for this reason, in morphine they are assigned between 1498 and 1400 cm^{-1}. In cocaine the rocking modes are predicted between 1194 and 1134 cm^{-1} [31] while in the tropane species [30] between 1183 and 1128 cm^{-1}, hence, in morphine these modes are predicted and assigned between 1177 and 1033 cm^{-1}.

TABLE – 3

Observed and calculated wavenumbers (cm^{-1}) and assignments for the free base, cationic and hydrochloride species of morphine in gas phase

Experimental			B3LYP/6-31G* Method[a]							
Free base		Hydroch.	Free base		Cationic		Hydrochloride		Dimer Hydrochloride	
FTIR[c]	FTIR[c]	Raman[d]	SQM[b]	Assignments	SQM[b]	Assignments	SQM[b]	Assignments	SQM[b]	Assignments
3545sh			3585	νO3-H40	3594	νO2-H39	3584	νO3-H40	3643	νO-H
3465sh			3549	νO2-H39	3586	νO3-H40	3556	νO2-H39		
3356s					3270	νN4-H41			3337	νO-H
		3287w							3216	νC-H
3207s,br		3206w,br							3201	νC-H
					3090	νC21-H38			3090	νC-H
					3080	ν_aCH_3	3082	νC21-H38		
			3078	νC21-H38	3072	νC17-H33				
3062sh			3063	νC17-H33	3064	νC19-H37	3068	νC17-H33	3067	ν_aCH_2
		3052m			3058	ν_aCH_3				
3052sh		3052m	3051	νC19-H37			3054	νC19-H37		
		3052m					3047	ν_aCH_3		
		3036s			3040	νC15-H32	3039	ν_aCH_3	3041	ν_sCH_2
		3036s	3029	νC15-H32	3036	ν_aCH_2(C12)	3034	νC15-H32		
		2989m					3008	ν_aCH_2(C12)	3005	νC-H
		2989m			2987	ν_aCH_2(C9)	2992	νC8-H24		
		2989m	2985	ν_aCH_3	2986	νC8-H24	2982	ν_aCH_2(C9)		

		2969s	2983	νC8-H24	2979	ν_sCH_2(C12)				
		2969s			2974	ν_sCH_3	2965	νC7-H23		
		2969s	2960	ν_aCH_2(C9)	2963	νC7-H23	2959	ν_sCH_3		
		2945vs			2951	ν_aCH_2(C11)	2952	ν_sCH_2(C12)		
2946m		2945vs	2943	ν_aCH_3			2943	ν_aCH_2(C11)		
		2945vs	2941	ν_aCH_2(C12)						
			2937	ν_aCH_2(C11)			2935	ν_sCH_2(C9)		
		2915m	2923	νC7-H23	2920	ν_sCH_2(C11)				
		2915m	2913	ν_sCH_2(C9)	2918	ν_sCH_2(C9)	2918	ν_sCH_2(C11)		
2907sh		2897m	2905	ν_sCH_2(C11)			2904	νC14-H31		
		2897m	2890	νC14-H31			2892	νC6-H22		
2863w		2865m	2887	νC6-H22	2843	νC14-H31				
2827w		2865m	2828	ν_sCH_3	2828	νC6-H22				
2724w			2821	ν_sCH_2(C12)						
2434w,br									2496	νN-H
1855w					1677	νC15-C17	1776	νN4-H41,νCl42-H41	1870	νN-H
1647w			1649	νC15-C17			1649	νC15-C17	1707	νC=C
		1641s	1638	νC10-C16	1638	νC10-C16	1637	νC10-C16	1684	νC=C
1616m		1614sh			1611	βR_2(A2)			1658	νC=C
		1594w	1609	νC13-C10,νC16-C20,			1609	νC16-C20,βR_2(A5)	1558	νC=C
1506sh			1506	νC21-C20	1511	νC21-C20,	1507	νC21-C20,βC19-H37	1509	δCH_2
1478s		1486w	1483	δaCH_3			1498	ρ'N4-H41,	1498	δaCH_3
1478s		1467w	1471	δCH_2(C12)	1473	δaCH_3	1468	δaCH_3,ρN4-H41,	1463	δsCH_3
1456s		1457sh	1456	νC10-C16,δCH_2(C11)	1461	δaCH_3	1459	δCH_2(C12),δaCH_3		
			1452	δaCH_3	1457	δCH_2(C12)	1455	βR_3(A4)		
1450sh					1452	βR_3(A4)	1450	δCH_2(C9)		
1444sh			1442	δCH_2(C9)	1447	δCH_2(C9)	1442	δCH_2(C12)	1443	ρC-H
1431w		1433w	1435	δCH_2(C11)	1437	δCH_2(C11)	1439	δCH_2(C11)	1435	ρC-H
			1424	δsCH_3	1428	ρN4-H41	1431	δaCH_3,τwH41-Cl42	1427	ρC-H
1416sh					1417	ρ'N4-H41			1419	ρC-H
					1407	βC15-H32,	1400	δsCH_3	1412	$wagCH_2$
1398w		1405m	1398	$wagCH_2$(C12)	1404	δsCH_3	1395	ρ'C14-H31	1396	$wagCH_2$
			1390	ρ'C14-H31,βC15-H32			1389	$wagCH_2$(C12)	1388	$wagCH_2$
					1380	$wagCH_2$(C12)	1378	δO2-H39,βC15-H32	1385	$wagCH_2$
1376w			1374	δO2-H39	1373	$wagCH_2$(C11)	1376	$wagCH_2$(C9)	1378	ρC-H
					1371	βC17-H33			1371	ρC-H
1366w			1367	ρC7-H23,$wagCH_2$(C9)	1367	$wagCH_2$(C9)			1370	ρC-H
1360sh			1361	$wagCH_2$(C11),ρ'C7-H23			1364	$wagCH_2$(C11)	1363	ρC-H
			1355	$wagCH_2$(C9),$wagCH_2$(C11)	1351	ρC7-H23,ρCH_2(C12)	1362	ρC7-H23	1362	ρC-H
1344sh		1349w	1348	ρ'C8-H24	1346	τO2-C14	1348	ρ'C8-H24	1346	ρC-H
					1344	νC13-C10	1344	ρ'C6-H22	1343	ρC-H
			1339	βC19-H37	1337	ρC14-H31	1340	νC13-C10,δO3-H40	1322	ρCH_2
1335m		1333w	1334	νC5-C10	1333	ρ'C8-H24	1334	ρC6-H22	1320	ρCH_2
			1316	ρC14-H31	1324	νC5-C10,νC20-O3	1316	νC19-C21,νC20-O3	1314	ρCH_2
1314m			1313	βC21-H38,νC20-O3	1314	ρC6-H22	1311	ρC14-H31	1312	ρCH_2
1289sh		1307w	1294	ρC6-H22					1294	δO-H
1282w		1275sh	1291	ρCH_2(C12),ρCH_2(C9)	1288	ρ'C6-H22,ρC8-H24	1284	ρCH_2(C9)	1287	ρCH_2
					1273	ρCH_2(C9)	1277	ρC8-H24	1278	δO-H
1264sh		1260w	1267	ρC8-H24,ρ'C6-H22	1261	ρCH_2(C11),ρ'C7-			1261	βC-H
1250s			1253	ρCH_2(C9)	1257	νC16-O1	1252	ρCH_2(C11),ρ'C7-H23	1256	βC-H
1237sh		1236w	1242	δO2C14C17			1245	δO2C14C17	1241	βC-H
1231sh			1238	ρCH_2(C11)	1232	βR_1(A5)	1235	ρCH_2(C12),νC5-C6	1235	βC-H
1227sh			1225	νC11-C13	1224	νC11-C13	1226	βR_1(A5),νC16-O1	1227	ρCH_2
1216w		1214w	1219	βR_1(A5)	1215	βR_1(A5)				
					1210	δO2-H39,ρ'C14-H31	1213	βR_1(A5),βR_2(A2)	1212	βC-H

1202m		1194w	1204	νC13-C19	1198	ρCH_2(C11),δO2-H39	1204	νC13-C19	1202	βC-H
1178sh			1180	ρCH_2(C11)	1185	ρCH_2(C11),τR_1(A3)	1187	ρCH_2(C11)	1194	ρCH_2
1170w			1170	βC17-H33,βC15-H32	1177	ρ'CH_3	1169	βC17-H33	1177	ρCH_3
1157w		1160w	1158	νN4-C18	1152	βC21-H38,	1154	νC5-C10	1153	βC-H
1148m			1148	νC19-C21			1149	βC21-H38	1148	νC-C
1142sh		1140w	1141	δO3-H40	1145	δO3-H40			1146	νC-C
1122s			1129	ρCH_3	1132	ρCH_3νC5-C8	1138	ρCH_3	1137	βR_2(A2)
			1117	νC5-C6			1114	δO2C14C17 βR_2(A2)	1115	βR_1(A5)
1111sh			1110	νC5-C9			1111	νC5-C9	1108	βR_1(A5)
		1102w			1106	βR_1(A5)	1106	νC5-C8	1097	νN-C
1098sh					1101	δO2C14C17			1095	νN-C
1076w			1087	νC5-C8,βR_2(A3)	1089	νC5-C9			1089	βR_2(A3)
		1062sh	1063	τR_1(A1),δO2C14C17	1074	νC14-O2	1064	νC14-O2	1079	βR_2(A3)
1053sh		1047s	1051	νC9-C12,νN4-C12,νC6-C7			1059	νN4-C18	1053	βR_2(A2)
1048w		1047s	1046	νC14-O2,νC17-C14			1048	νC17-C14	1045	τR_1(A3)
1039sh					1041	ρCH_3,τR_1(A3)	1041	νC6-C7,νC7-C11	1041	τR_1(A3)
1026sh			1033	ρ'CH_3	1027	νC6-C7,νC7-C11			1038	τR_2(A1)
					1024	δO2C14C8,τR_2(A1)			1000	τR_2(A1)
1014sh		1011w	1012	νC6-C15,νC8-C14	1004	τR_1(A1),τO2-C14	1011	νC9-C12	1000	τR_1(A1)
		997sh	999	νC16-O1	994	γC17-H33	1006	νC6-C15,νN4-C12	994	τwCH_2
981m					984	νN4-C18,νC6-C15	992	τR_1(A1)	993	τwCH_2
			978	γC17-H33,γC15-H32	970	νC9-C12	977	γC17-H33,γC15-H32	984	γC-H
963w		965w	961	δO2C14C17,νC9-C12	963	τR_2(A1),δO2C14C8	963	δO2C14C17 βR_2(A2)	963	γC-H
945s		947w	953	τR_2(A1),τR_1(A3)	940	τR_2(A1),δO2C14C17	947	νN4-C7,βR_3(A4)	947	τR_2(A1)
939sh			934	τR_2(A1),τR_1(A1)	938	γC19-H37,γC21-H38	932	τR_2(A1) δO2C14C17	942	τR_2(A1)
923w		921w	925	δO2C14C8	920	τR_1(A4)	921	γC21-H38,γC19-H37	930	τwCH_2
			919	γC19-H37			913	τwCH_2(C12)	917	γC-H
		907sh	908	τwCH_2(C11)	897	τwCH_2(C12)			901	τR_1(A4)
887w					886	τwCH_2(C9)	898	τR_1(A4),τwCH_2(C11)	889	τwCH_2
876w		869sh	867	βR_3(A4),τR_1(A4)			864	τR_3(A1),τR_2(A1)		
845sh		854w	852	νC8-O1,νC7-C11	854	νC8-O1,νN4-C12	859	βR_3(A4),δO2C14C8	845	νC-O1
835s					843	γC15-H32			843	νC-C
815sh		820w	824	τO2-C14τR_3(A1)	820	νC8-C14	827	νC8-O1,νC8-C14	826	τwCH_2
804vs		798sh	808	γC21-H38	815	γC19-H37,γC21-H38	807	γC21-H38,γC19-H37	815	γC-H
788w		784w	778	τwCH_2(C9),τwCH_2(C12)					796	γC-H
769sh			775	δO2C14C8,τR_1(A1)	776	δO2C14C8	775	δO2C14C8,τR_1(A1)	783	τR_1(A1)
762m		758m			761	βR_1(A5)	770	τwCH_2(C9)	758	τR_1(A1)
750sh			742	νN4-C7	741	τR_1(A1) δO2C14C17	754	νN4-C7	756	τR_1(A5)
		740sh	732	τR_2(A4),τR_1(A5)			730	τR_2(A4),τR_1(A5)		
719w					717	νN4-C7			718	τR_2(A4)
707w		702sh			701	τR_1(A5),τR_2(A4)			711	γC-H
707w		702sh	697	βR_3(A5),βR_1(A5)	696	βR_2(A5)	697	βR_3(A5),βR_3(A4)		
			692	τR_1(A5)			691	τR_1(A5)	680	βR_3(A5)
680sh		688m			685	δO2C14C8			678	γC-H
673w			666	βR_1(A2)βR_2(A4)			665	βR_1(A2)	671	τO-H---Cl
655w		655w	641	δO2C14C8			645	δO2C14C8	656	γC-H
		633sh			632	δO2C14C8,τR_1(A1)			630	τR_1(A1)
		615vs	608	δO2C14C8,βR_2(A2)	602	δO2C14C8,τO2-C14	608	δO2C14C8,βR_2(A2)	613	δOCC
		581m	593	τR_2(A5),γC20-O3	596	τR_2(A5),γC20-O3	596	τR_2(A5),γC20-O3	592	γC-O
		569sh	575	τR_2(A4),βR_3(A4)	577	βR_3(A4),τR_1(A4)	576	τR_2(A4)	573	βR_3(A4)
		563sh	556	βR_2(A2)	561	τO2-C14,βR_2(A2)	556	βR_2(A2)	550	βR_2(A2)
			539	τR_3(A5),τR_1(A2)	536	τR_3(A5),τR_1(A2)	535	τR_3(A5),τR_1(A2)	539	τR_1(A2)
		527sh	525	βR_2(A2),βR_3(A5)	523	δO2C14C8,τR_2(A1)	524	βR_2(A2),βR_3(A5)	535	βR_2(A2)
	497w	509m					515	γN4-C18	512	τO-H---Cl
	491w		493	τO2-C14,δO2C14C8	504	γN4-C18			490	τO-H---Cl
	482w		481	βR_3(A5)	479	βR_3(A5)	485	βR_3(A5)	490	βR_3(A5)

	470sh				473	δO2C14C17,τR_3(A1)			469	δOCC
	465sh	466m	464	δO2C14C17,βR_3(A4)			461	δO2C14C17,	467	βR_3(A4)
	456m				450	βR_2(A1)			451	δOCC
	441m	446m	445	δO2C14C17,βR_2(A1)			442	βR_2(A1)	443	δOCC
	431w				436	βR_3(A1)	433	βR_3(A1)	442	δOCC
	419m	420s	426	βR_3(A4),βR_3(A1)					408	τO-H
	400m		396	τR_1(A1),βR_3(A3)			395	τR_1(A1),βR_3(A3)	400	βR_3(A3)
	386w		386	τO2-H39	384	τR_1(A1),βR_3(A3)			398	τO-H
	375m	372s			371	δO2C14C8	373	τO2-H39	372	βN-C
	362w	358s	360	τO2-C14,δO2C14C17			364	δO2C14C17,	363	τO-H
	351m				353	δO2C14C17	353	τO2-C14,	354	δCCC
	345w	332s	343	τR_2(A4),τR_1(A4),τR_3(A4)	343	τO2-C14			344	τR_2(A4)
	335m				336	τO3-H40	339	τR_3(A4)		
	327m		329	τR_1(A3), γN4-C18					325	τR_3(A4)
	323m		320	τO3-H40	322	τR_1(A3)	324	τO3-H40	323	τR_1(A3)
	315w	312sh	318	τO2-C14, τO3-H40	310	ρN4-C18	314	τR_2(A3)	315	ρN4-C18
	303m	300s	299	τO2-C14,τR_1(A1)	297	τO2-C14	301	βR_2(A3),βN4-C18	299	ρN4-C18
	281m	274w	272	τO2-C14,δO2C14C8			275	τO2-C14,δO2C14C8	279	τO-C
	266w				266	τR_2(A3),βR_2(A3)			266	τR_2(A3)
	257sh				257	βC20-O3	258	τR_1(A3)	261	τwCH_3
	253m	254w	252	τR_2(A3)	251	τO2-C14,τR_3(A1)			251	τO-C
	245m		244	βC20-O3,τR_2(A2)			244	τR_2(A1),βC20-O3	244	τwCH_3
	231m	233w	234	τO2-C14,δO2C14C8			237	τO2-C14,δO2C14C8		
	227m	222sh	222	τwCH_3						
	214m								219	γC-O
	209m				207	τR_2(A1),τwCH_3	209	δO2C14C17,	206	δCCC
	203m		202	τR_3(A1)	205	τR_2(A1)			200	τR_2(A1)
	195w	191w					199	τO2-C14,τR_3(A1)	197	τR_3(A1)
	188w				188	τO2-H39	183	τwCH_3,τR_3(A3)		
	170m	167sh	157	τR_3(A3)	154	τO2-C14,τR_3(A1)			173	τR_3(A3)
		149sh					149	τR_3(A1)	150	τR_3(A1)
			121	τO2-C14,τR_2(A1)			123	τO2-C14	127	τO-C
			115	τO2-C14	114	τR_3(A4)	115	τO2-C14	118	νCl---H
					100	τO2-C14,τR_3(A1)	75	τO2-C14,τR_2(A1)	82	νCl---H
			69	τO2-C14,τR_2(A4)	64	τO2-C14,τR_3(A4)	68	τO2-C14,τR_2(A1)	73	τR_3(A4)
			54	τR_2(A1)			45	τO2-C14,τR_2(A1)	47	τR_2(A1)
							41	τO2-C14,τR_2(A1)	37	νCl---H
					33	τO2-C14			33	τO-C

Abbreviations: br, broad; ν, stretching; β, deformation in the plane; γ, deformation out of plane; wag, wagging; τ, torsion; β_R, deformation ring τ_R, torsion ring; ρ, rocking; τw, twisting; δ, deformation; a, antisymmetric; s, symmetric; (A_1), Ring1; (A_2), Ring2; (A_3), Ring3; (A_4), Ring4; (A_5), Ring5.

[a]This work, [b]From scaled quantum mechanics force field; [c]From Ref [23]; [d]From Ref [24]

The twisting modes in the tropane species were assigned between 205 and 151 cm^{-1} while in cocaine they were assigned between 191 and 117 cm^{-1}, as predicted by calculations. In morphine, these modes were assigned between 244 and 183 cm^{-1}, as predicted by the SQM calculation s for the three species. In other species with CH_3 groups these modes were assigned in the similar regions [35,36,51,52].

CH_2 modes. Each morphine species presents three CH_2 groups two of which are located in the R3 rings and the other one in the R4 rings, as observed in Figures 1 and 2. Hence, a total of six antisymmetric and symmetric stretching modes and three deformations, waging, rocking and twisting modes are expected in each free base, cationic and hydrochloride morphine species. For instance, in cocaine the stretching modes are predicted in the 3009-2938 cm^{-1} range [31] although in tropane species these modes are predicted between 3024 and 2911 cm^{-1} [30]. In morphine, we observed that these two antisymmetric CH_2 stretching modes corresponding to the C9 and C12 atoms belong to the R3 rings are predicted at higher wavenumbers when these are compared with the corresponding antisymmetric modes belong to the C11 atoms of the R4 rings. Here, it is indispensable to clarify that the symmetric modes for the cationic species are predicted with higher intensities in the Raman spectrum than the corresponding to the other species. Hence, these stretching modes for those three morphine species are assigned respectively to the bands observed in the 2960-2821, 3036-2918 and 3008-2918 cm^{-1} regions, as predicted by the calculations. The deformation, wagging, rocking and twisting modes in the tropane species were assigned respectively to the bands between 1485/1442, 1385/1274, 1274/1142 and 967/639 cm^{-1} [30] while in cocaine are predicted in the 1483/1449, 1382/1242, 1230/1167 and 933/744 cm^{-1} regions [31]. Here, the SQM calculations have predicted the deformation, wagging, rocking and twisting modes of these groups in the 1509-1435, 1412-1355, 1351-1180 and 930-770 cm^{-1} regions and, for these reasons, they are assigned to the bands located in these regions, as indicated in Table 3.

Skeletal modes. For the three morphine species it is very important to analyze the N-CH_3 stretching modes because these groups play a very significant role in the pharmacological and medicinal properties of the tropane alkaloids, as was reported in the literature [8-19]. These stretching modes in the tropane species were assigned to the IR bands at 1128, 1086 and 1031 cm^{-1} while in the three cocaine species were predicted at 1113, 1058 and 1052 cm^{-1}. In the free base of morphine that mode was predicted at 1158 cm^{-1}, in the cationic form at 984 cm^{-1} and in the hydrochloride form at 1059 cm^{-1}, hence, these modes can be easily assigned to the Raman bands at 1160, 984 and 1047 cm^{-1}, respectively. The other two N-C stretching modes corresponding to the R3 rings are predicted in the free base, cationic and hydrochloride morphine species at 1051/742, 854/717 and 1006/947 cm^{-1}, respectively and, therefore, they were assigned in those regions. These vibration modes

in the three tropane species [30] were assigned at 981, 776, 729, 706 and 680 cm^{-1} while in cocaine were assigned at 951/777, 922/747, 786/731 cm^{-1} [31]. On the other hand, the C-O stretching corresponding to the furane rings are predicted in different regions, thus, in the free base of morphine both modes were predicted at 997/854 cm^{-1}, in the cationic form at 1257,854 cm^{-1} and in the hydrochloride form at 1226/827 cm^{-1}, hence, these modes were easily assigned to IR and Raman bands in these regions.

Here, it is necessary to clarify that in the six members rings are normally expected three deformations (β_{R1}(A1), β_{R2}(A1) and β_{R3}(A1)) and three torsions ($_{R1}$(A1), $_{R2}$(A1) and $_{R3}$(A1)) rings modes while in five members rings only two deformation and torsion rings modes are expected. But, when there are three atoms common to two rings, as in tropane and cocaine where in each species it is observed only three atoms common, the redundant internal coordinates should be removed. Hence, in morphine, due to the three pairs of atoms common to two rings of the five present in the three structures of morphine, only two redundant internal coordinates were identified and removed, these were the deformation βR_1(A1) and βR_1(A3) modes corresponding to the R1 and R3 rings. Hence, a total of twenty five deformation and torsion rings modes are expected for all morphine species which were assigned as predicted by SQM calculations and, as observed in Table 3. The skeletal modes remain were assigned in accordance to the contributions PED observed by the calculations.

FORCE FIELDS

From the force fields computed for the three species of morphine in gas and aqueous solution phases by using the B3LYP/6-31G* method with the SQMFF methodology [28] and the Molvib program [29] were obtained the scaled internal force constants which are summarized in **Table 4** together with the reported for the species of tropane and cocaine alkaloids in both media by using the same level of theory. Comparing first the *f(O-H)* force constants for the species of morphine it is observed that they are different in gas phase but in solution the values for the cationic and hydrochloride species slightly decrease probably due to the hydration while the corresponding to the free base practically do not change. For the free base it is observed nearly the same behaviours in both media, as supported by the low volume variation in solution, low dipole moment value, low solvation energy and, few change in the geometrical parameters (Tables 1 and 2). In **Figure S16** are presented the comparisons among the force constants for those three different alkaloids in both media. First, regarding the values for the free base in both media the same behaviours are observed in both media and showing approximately the same values for the *f(νN-H), f(νN-CH$_3$), f(νCH$_2$), f(νCH$_3$)* and *f(νC-H)* constants with exception of the *f(νC-N)* and *f(νC-C)* constants that for the free base of morphine in both media have higher values that the corresponding to tropane and cocaine. In the three different alkaloids the *f(δCH$_2$)* and *f(δCH$_3$)* constants have basically the same values. In the cationic species of the three alkaloids are observed different *f(νN-H)* constants values in gas phase but in solution have the same values. The *f(νC-C)* constants for the cationic species of morphine in both media have also higher values than the corresponding to tropane and cocaine. For the hydrochloride species of the three alkaloids the *f(νN-CH$_3$)* constant in gas phase is higher than *f(νN-H)* and *f(νC-N)* but in solution *f(νN-H) > f(νN-CH$_3$) > f(νC-N)* and, on the other hand, the *f(νC-C)* constants for morphine in both media present the higher values than the other two alkaloids.

TABLE – 4

Scaled internal force constants for the free base, cationic and hydrochloride morphine species compared with the corresponding to cocaine and tropane species in gas and aqueous solution phases.

B3LYP/6-31G*						
Morphine[a]						
Force constant	Free base		Cationic		Hydrochloride	
	Gas	PCM	Gas	PCM	Gas	PCM
f(νO-H)	7.12	7.13	7.21	7.13	7.13	7.05
f(νN-H)			5.93	5.98	2.73	4.61
f(νN-CH$_3$)	4.83	4.69	4.05	4.15	4.37	4.25
f(νC-N)	4.74	4.59	3.67	3.91	4.20	4.03
f(νCH$_2$)	4.69	4.72	4.85	4.90	4.82	4.89
f(νCH$_3$)	4.70	4.76	5.08	5.12	5.01	5.09
f(νC-H)	4.65	4.71	4.62	4.77	4.72	4.79
f(νC-C)	5.74	5.73	6.04	5.77	5.79	5.78
f(δCH$_2$)	0.74	0.73	0.73	0.72	0.73	0.72
f(δCH$_3$)	0.58	0.57	0.56	0.56	0.56	0.56
Cocaine[b]						
Force constant	Free base		Cationic		Hydrochloride	
	Gas	PCM	Gas	PCM	Gas	PCM
f(νN-H)			4.91	5.55	3.23	4.79
f(νN-CH$_3$)	4.69	4.52	4.17	4.23	4.31	4.17
f(νC-N)	4.20	4.01	3.41	3.51	3.71	3.54
f(νCH$_2$)	4.85	4.87	4.91	4.93	4.88	4.93
f(νCH$_3$)	4.86	4.92	5.07	5.09	5.04	5.08
f(νC-H)	4.86	4.91	4.93	5.02	4.91	4.98
f(νC-C)	3.94	3.98	4.06	4.09	4.08	4.11
f(δCH$_2$)	0.74	0.72	0.75	0.73	0.75	0.73
f(δCH$_3$)	0.58	0.56	0.57	0.56	0.57	0.56
Tropane[c]						
Force constant	Free base		Cationic		Hydrochloride	
	Gas	PCM	Gas	PCM	Gas	PCM
f(νN-H)			5.97	5.98	2.70	4.69
f(νN-CH$_3$)	4.69	4.52	4.09	4.21	4.42	4.26
f(νC-N)	4.16	3.97	3.11	3.35	3.73	3.48
f(νCH$_2$)	4.78	4.78	4.88	4.88	4.85	4.87
f(νCH$_3$)	4.72	4.79	5.10	5.13	5.03	5.11
f(νC-H)	4.78	4.82	4.92	4.99	4.90	4.96
f(νC-C)	4.05	4.06	4.17	4.21	4.16	4.20
f(δCH$_2$)	0.74	0.72	0.75	0.72	0.74	0.73
f(δCH$_3$)	0.58	0.57	0.56	0.56	0.56	0.56

Units are mdyn $Å^{-1}$ for stretching and mdyn Å rad^{-2} for angle deformations, [a]This work; [b]From Ref [30]; [c]From Ref [31]

A result very important is that the behaviours of all constants for the three species of tropane and cocaine are practically similar for the free base but slight changes are observed for the cationic and hydrochloride species and, the most important difference observed with morphine is in the *f(C-N)* and *f(C-C)* values because the two are higher in both media than the corresponding to tropane and cocaine.

CONCLUSIONS

In the present work, the theoretical structures of the free base, cationic and hydrochloride species of morphine were determined in gas phase and in aqueous solution by using the hybrid B3LYP/6-31G* method while the solvent effects were considered with the SCRF and PCM methods employing the SMD model. Here, the MK and NPA charges, the molecular electrostatic potential surfaces, bond orders and stabilization energies were studies for the three morphine species. In particular, the NBO and AIM analyses reveal clearly the high stability of the hydrochloride species of morphine than the other ones. The studies by using the frontier orbitals evidence that the cationic species of morphine is the most reactive in gas phase while the hydrochloride species in aqueous solution. Hence, the free base is the less reactive species of morphine in both media. The descriptors show that the cationic species of morphine in both media present the higher electrophilic and nucleophilic indexes than the other ones. The force fields for the free base, cationic and hydrochloride structures of morphine were computed and the complete vibrational assignments for their expected 114, 117 and 120 vibration normal modes, respectively were here reported for first time together to their force constants.

The comparisons of the three species of morphine with the tropane and cocaine alkaloids support that: (i) the morphine species present higher dipole moment values in both media and higher solvation energies are observed for their cationic and hydrochloride forms in relation to the cocaine ones while the cocaine species are more voluminous than the morphine ones, (ii) the high stabilities of the three morphine species than the cocaine ones are clearly revealed by the higher total energies of their three species, (iii) the NBO study evidence that the three morphine species have higher total energies than the corresponding to cocaine, (vi) the AIM study reveals clearly that the differences fundamental among the three forms of morphine than cocaine are the O---O interactions observed only for cocaine in both media, generating instability in their hydrochloride cocaine species and, (v) the frontier orbitals suggest that in the cocaine and tropane alkaloids the cationic forms are the less reactive and, as a consequence the most stable. The most important results observed in this study are that in aqueous solution, the hydrochloride forms of the three alkaloids are the most reactive being cocaine most reactive than morphine. Probably, the lower reactivities observed for the free base and hydrochloride

morphine species than cocaine ones could be explained by the five different rings present in morphine and, also, probably because cocaine present the higher electrophilic and nucleophilic indexes.

ACKNOWLEDGEMENTS

This work was supported with grants from CIUNT Project Nº 26/D207 (Consejo de Investigaciones, Universidad Nacional de Tucumán). The author would like to thank Prof. Tom Sundius for his permission to use MOLVIB.

Supporting Information Available: Tables S1-S6 and **Figures S1-S16**.

Supporting Material

Table S1. Atomic MK charges and molecular electrostatic potentials for the most stable free base, cationic and hydrochloride structures of cocaine by using the hybrid B3LYP/6-31G* level of theory.

Atoms	MK charges						MEP					
	Free base		Cationic		Hydrochloride		Free base		Cationic		Hydrochloride	
	Gas	PCM	Gas	PCM	Gas	PCM	Gas	PCM	Gas	PCM	Gas	PCM
1 O	-0.321	-0.439	-0.414	-0.435	-0.342	-0.334	-22.275	-22.290	-22.170	-22.175	-22.260	-22.256
2 O	-0.654	-0.598	-0.570	-0.576	-0.640	-0.641	-22.321	-22.313	-22.213	-22.211	-22.311	-22.307
3 O	-0.508	-0.539	-0.513	-0.509	-0.515	-0.520	-22.283	-22.293	-22.184	-22.191	-22.267	-22.263
4 N	-0.313	-0.328	-0.041	-0.008	0.338	0.338	-18.355	-18.357	-18.063	-18.059	-18.247	-18.225
5 C	0.439	0.064	-0.049	-0.126	0.218	0.273	-14.714	-14.718	-14.581	-14.578	-14.693	-14.687
6 C	-0.092	0.053	0.178	0.275	0.094	0.065	-14.726	-14.728	-14.573	-14.572	-14.705	-14.697
7 C	0.158	0.075	-0.120	-0.110	0.042	-0.034	-14.701	-14.704	-14.520	-14.519	-14.656	-14.646
8 C	-0.203	0.354	0.284	0.405	-0.081	-0.111	-14.673	-14.677	-14.556	-14.556	-14.658	-14.653
9 C	-0.348	-0.337	-0.297	-0.210	-0.089	-0.089	-14.734	-14.737	-14.584	-14.580	-14.711	-14.701
10 C	-0.295	-0.225	-0.136	-0.244	-0.344	-0.339	-14.749	-14.756	-14.631	-14.631	-14.729	-14.722
11 C	-0.245	-0.178	-0.115	-0.143	-0.391	-0.325	-14.733	-14.736	-14.584	-14.582	-14.696	-14.689
12 C	0.030	0.072	0.030	-0.016	-0.175	-0.146	-14.713	-14.716	-14.528	-14.525	-14.667	-14.655
13 C	0.253	0.236	0.200	0.218	0.320	0.296	-14.737	-14.742	-14.617	-14.617	-14.714	-14.708
14 C	0.503	0.295	0.231	0.220	0.446	0.469	-14.680	-14.675	-14.565	-14.563	-14.669	-14.664
15 C	-0.196	-0.328	-0.375	-0.468	-0.268	-0.245	-14.741	-14.742	-14.617	-14.617	-14.725	-14.720
16 C	0.225	0.235	0.203	0.271	0.254	0.234	-14.692	-14.699	-14.582	-14.582	-14.674	-14.667
17 C	-0.287	-0.127	-0.078	-0.002	-0.242	-0.268	-14.747	-14.745	-14.624	-14.625	-14.734	-14.728
18 C	-0.329	-0.303	-0.410	-0.440	-0.430	-0.436	-14.717	-14.720	-14.526	-14.523	-14.669	-14.660
19 C	-0.323	-0.330	-0.331	-0.338	-0.347	-0.341	-14.743	-14.749	-14.632	-14.633	-14.723	-14.717
20 C	0.165	0.203	0.240	0.199	0.194	0.201	-14.679	-14.686	-14.571	-14.574	-14.661	-14.654
21 C	-0.186	-0.208	-0.211	-0.168	-0.201	-0.200	-14.742	-14.748	-14.637	-14.638	-14.724	-14.718
22 H	0.053	0.052	0.033	0.005	0.038	0.047	-1.119	-1.120	-0.965	-0.963	-1.099	-1.092
23 H	0.072	0.090	0.124	0.120	0.083	0.111	-1.120	-1.123	-0.941	-0.939	-1.076	-1.067
24 H	0.114	-0.016	0.041	0.001	0.097	0.103	-1.106	-1.106	-0.988	-0.987	-1.093	-1.087
25 H	0.083	0.092	0.095	0.065	0.045	0.044	-1.121	-1.122	-0.968	-0.965	-1.101	-1.091
26 H	0.120	0.121	0.163	0.151	0.088	0.086	-1.118	-1.120	-0.968	-0.964	-1.092	-1.083
27 H	0.076	0.066	0.117	0.121	0.140	0.132	-1.116	-1.120	-0.972	-0.971	-1.083	-1.075
28 H	0.095	0.080	0.065	0.069	0.108	0.097	-1.115	-1.118	-0.968	-0.964	-1.079	-1.070
29 H	0.037	0.039	0.081	0.108	0.072	0.069	-1.130	-1.132	-0.940	-0.935	-1.077	-1.064
30 H	0.095	0.084	0.104	0.105	0.127	0.124	-1.120	-1.123	-0.935	-0.932	-1.075	-1.064
31 H	0.019	-0.026	0.011	-0.002	0.042	0.042	-1.114	-1.113	-1.008	-1.000	-1.104	-1.098
32 H	0.132	0.157	0.182	0.203	0.153	0.157	-1.108	-1.108	-0.985	-0.984	-1.092	-1.086
33 H	0.143	0.135	0.159	0.146	0.145	0.151	-1.111	-1.111	-1.000	-0.997	-1.099	-1.094
34 H	0.099	0.094	0.208	0.216	0.141	0.152	-1.125	-1.125	-0.926	-0.922	-1.066	-1.057
35 H	0.127	0.125	0.191	0.194	0.165	0.176	-1.116	-1.118	-0.924	-0.922	-1.067	-1.059
36 H	0.136	0.129	0.178	0.187	0.174	0.181	-1.118	-1.120	-0.924	-0.921	-1.070	-1.061
37 H	0.153	0.153	0.178	0.176	0.169	0.168	-1.112	-1.118	-1.004	-1.005	-1.092	-1.087
38 H	0.173	0.179	0.209	0.197	0.184	0.187	-1.109	-1.115	-1.009	-1.010	-1.092	-1.087
39 H	0.402	0.377	0.401	0.397	0.397	0.398	-1.004	-0.994	-0.895	-0.893	-0.993	-0.990
40 H	0.399	0.422	0.437	0.433	0.408	0.411	-0.968	-0.979	-0.871	-0.879	-0.953	-0.950
41 H			0.316	0.312	0.013	0.029			-0.810	-0.805	-0.987	-0.980
42 Cl					-0.629	-0.713					-64.506	-64.528

Table S2. NPA charges and Wiberg indexes for the most stable free base, cationic and hydrochloride structures of morphine by using the hybrid B3LYP/6-31G* level of theory.

Atoms	MK charges						MEP					
	Free base		Cationic		Hydrochloride		Free base		Cationic		Hydrochloride	
	Gas	PCM	Gas	PCM	Gas	PCM	Gas	PCM	Gas	PCM	Gas	PCM
1 O	-0.569	-0.548	-0.545	-0.532	-0.565	-0.561	2.061	2.076	2.073	2.092	2.067	2.068
2 O	-0.750	-0.738	-0.733	-0.728	-0.745	-0.744	1.795	1.802	1.815	1.813	1.800	1.799
3 O	-0.688	-0.693	-0.666	-0.672	-0.683	-0.686	1.921	1.912	1.957	1.943	1.929	1.923
4 N	-0.515	-0.510	-0.451	-0.448	-0.497	-0.484	3.118	3.110	3.472	3.473	3.354	3.388
5 C	-0.092	-0.089	-0.094	-0.092	-0.093	-0.093	4.003	4.004	4.003	4.004	4.004	4.004
6 C	-0.285	-0.286	-0.288	-0.292	-0.303	-0.305	3.943	3.944	3.946	3.944	3.920	3.921
7 C	-0.047	-0.049	-0.033	-0.035	-0.042	-0.041	3.927	3.928	3.853	3.852	3.884	3.875
8 C	0.096	0.095	0.091	0.093	0.097	0.097	3.834	3.850	3.839	3.849	3.829	3.830
9 C	-0.450	-0.451	-0.477	-0.476	-0.471	-0.472	3.900	3.900	3.879	3.881	3.878	3.879
10 C	-0.076	-0.080	-0.101	-0.102	-0.080	-0.080	3.987	3.987	3.982	3.981	3.986	3.986
11 C	-0.491	-0.491	-0.492	-0.492	-0.488	-0.490	3.893	3.893	3.875	3.876	3.887	3.885
12 C	-0.260	-0.263	-0.257	-0.258	-0.261	-0.259	3.867	3.868	3.777	3.780	3.816	3.811

13 C	-0.044	-0.045	-0.078	-0.073	-0.058	-0.058	3.993	3.993	3.989	3.989	3.993	3.993
14 C	0.049	0.053	0.046	0.047	0.046	0.044	3.879	3.877	3.878	3.884	3.876	3.876
15 C	-0.215	-0.210	-0.247	-0.242	-0.221	-0.220	3.950	3.949	3.939	3.937	3.947	3.947
16 C	0.255	0.263	0.261	0.269	0.259	0.258	3.904	3.909	3.910	3.910	3.906	3.908
17 C	-0.244	-0.233	-0.186	-0.192	-0.235	-0.235	3.953	3.951	3.942	3.940	3.952	3.951
18 C	-0.466	-0.469	-0.475	-0.473	-0.474	-0.472	3.815	3.816	3.714	3.714	3.753	3.743
19 C	-0.231	-0.235	-0.223	-0.227	-0.230	-0.229	3.947	3.947	3.941	3.942	3.945	3.945
20 C	0.280	0.279	0.306	0.299	0.286	0.285	3.916	3.917	3.922	3.924	3.918	3.919
21 C	-0.271	-0.270	-0.252	-0.250	-0.267	-0.265	3.945	3.945	3.940	3.939	3.944	3.944
22 H	0.269	0.267	0.254	0.252	0.302	0.303	0.932	0.933	0.939	0.940	0.913	0.913
23 H	0.249	0.249	0.273	0.275	0.271	0.277	0.940	0.941	0.928	0.927	0.929	0.926
24 H	0.246	0.233	0.251	0.244	0.253	0.254	0.942	0.949	0.939	0.943	0.939	0.938
25 H	0.238	0.236	0.249	0.247	0.276	0.273	0.946	0.947	0.940	0.942	0.927	0.929
26 H	0.248	0.249	0.289	0.288	0.259	0.263	0.941	0.940	0.919	0.919	0.935	0.933
27 H	0.253	0.252	0.288	0.286	0.268	0.271	0.938	0.938	0.919	0.920	0.930	0.929
28 H	0.248	0.247	0.256	0.252	0.249	0.249	0.940	0.941	0.936	0.938	0.940	0.940
29 H	0.206	0.207	0.271	0.270	0.241	0.244	0.963	0.962	0.929	0.929	0.945	0.943
30 H	0.239	0.239	0.267	0.268	0.266	0.269	0.945	0.945	0.930	0.930	0.932	0.930
31 H	0.242	0.218	0.236	0.230	0.253	0.255	0.945	0.956	0.948	0.951	0.939	0.937
32 H	0.233	0.234	0.247	0.247	0.235	0.237	0.948	0.947	0.941	0.940	0.946	0.946
33 H	0.243	0.248	0.265	0.270	0.247	0.250	0.943	0.940	0.932	0.929	0.941	0.940
34 H	0.190	0.191	0.261	0.260	0.229	0.229	0.969	0.968	0.933	0.933	0.949	0.949
35 H	0.226	0.226	0.263	0.263	0.252	0.259	0.950	0.950	0.932	0.932	0.938	0.935
36 H	0.229	0.229	0.264	0.264	0.263	0.267	0.949	0.949	0.931	0.931	0.933	0.931
37 H	0.236	0.234	0.249	0.247	0.238	0.239	0.946	0.947	0.939	0.940	0.945	0.944
38 H	0.248	0.247	0.266	0.267	0.252	0.254	0.940	0.940	0.931	0.930	0.938	0.937
39 H	0.479	0.472	0.486	0.483	0.479	0.478	0.773	0.779	0.766	0.768	0.774	0.774
40 H	0.493	0.495	0.501	0.503	0.496	0.496	0.759	0.756	0.751	0.748	0.756	0.755
41 H			0.460	0.461	0.412	0.457			0.792	0.791	0.840	0.803
42 Cl					-0.714	-0.814					0.508	0.345

Table S3. Main donor-acceptor energy interactions (in kJ/mol) for the free base, cationic and hydrochloride structures of morphine and cocaine by using the hybrid B3LYP/6-31G* level of theory.

MORPHINE						
Delocalization	Free base		Cationic		Hydrochloride	
	Gas	PCM	Gas	PCM	Gas	PCM
*N4-C7 LP*H41*					47,38	59,36
*N4-C12 LP*H41*					51,58	59,20
*N4-C18 LP*H41*					54,00	65,10
ET_{LP*}					**152,96**	**183,66**
*(2)C10-C13*C16-C20*	89,90	88,15	77,04	78,37	85,74	84,12
*(2)C10-C13*C19-C21*	81,16	79,25	73,96	72,30	79,66	78,71
*(2)C16-C20*C10-C13*	87,61	87,36	97,76	95,56	91,02	90,40
*(2)C16-C20*C19-C21*	78,79	81,04	75,38	77,79	78,58	78,46
(2)C19-C21 C10-C13*	73,22	73,80	77,75	79,16	73,76	74,26
(2)C19-C21 C16-C20*	78,29	76,38	78,79	78,42	78,08	77,83
ET_{*}	**488,97**	**485,97**	**480,69**	**481,60**	**486,84**	**483,77**
** C16-C20*C10-C13*	764,44	896,73			1040,46	1069,04
** C19-C21*C10-C13*	950,27	992,66				
ET_{**}	**1714,71**	**1889,39**			**1040,46**	**1069,04**
*LP(2)O1 * C16-C20*	97,51	103,42	92,10	102,96	100,09	99,13
*LP(2)O3 * C16-C20*	111,28	106,29	126,34	116,19	114,65	110,53
ET_{LP*}	**208,79**	**209,71**	**218,44**	**219,15**	**214,74**	**209,66**
*LP(1)N4 LP*H41*					1238,02	1473,60
*LP(4)Cl42 LP*H41*					669,88	291,08
$ET_{LP LP*}$					**1907,90**	**1764,67**
E_{Total}	**2412,47**	**2585,07**	**699,13**	**700,75**	**3802,91**	**3710,81**
COCAINE						
Delocalization	Free base		Cationic		Hydrochloride	
	Gas	PCM	Gas	PCM	Gas	PCM
*N5-C6 LP*H44*					44.81	54.30
*N5-C7 LP*H44*					58.94	60.99
*N5-C13 LP*H44*					63.54	69.26
ET_{LP*}					**167.29**	**184.55**
*(2)C17-C19*O4-C15*	95.55	96.56	110.94	107.51	99.23	102.74
*(2)C17-C19*C18-C20*	87.61	87.32	82.56	82.60	88.45	88.16
*(2)C17-C19*C21-C22*	77.46	77.58	71.27	71.81	76.33	75.45
(2)C18-C20 C17-C19*	78.79	78.29	80.51	81.01	77.75	77.08
*(2)C18-C20*C21-C22*	90.20	90.16	89.79	89.66	89.70	89.54
(2) C21-C22 C17-C19*	92.88	93.30	101.53	100.19	94.26	95.51
*(2) C21-C22*C18-C20*	76.12	75.95	73.23	73.86	76.20	76.03
ET_{*}	**598.62**	**599.16**	**609.82**	**606.64**	**601.92**	**604.51**
**O4-C15* C17-C19*	385.94	384.27	279.22	260.08	304.01	287.33
** C17-C19*C18-C20*			890.55	890.88		

ET_{**}	**385.94**	**384.27**	**1169.77**	**1150.96**	**304.01**	**287.33**
*LP(2)O1 *O4-C15*	205.36	210.13	165.15	183.13	194.29	36.41
*LP(2)O2 *O3-C14*	200.97	209.04	264.05	250.09	200.47	206.49
*LP(2)O3 *O2-C14*	145.34	137.69	118.59	124.77	140.78	136.39
*LP(2)O3 *N5-C14*			75.16	42.85		
*LP(2)O3 *C8-C14*	81.64	78.63	56.85	64.54	88.57	89.12
*LP(2)O4 *O1-C15*	137.02	132.13	152.49	141.49	139.03	134.60
*LP(2)O4 *C15-C17*	75.24	73.28	70.73	70.68	73.53	72.19
ET_{LP*}	**845.57**	**840.89**	**903.01**	**877.55**	**836.67**	**675.20**
*LP(1)N5 LP*H44*					1323.30	1540.71
*LP(4)Cl45 LP*H44*					494.24	244.49
$ET_{LP LP*}$					**1817.54**	**1785.20**
E_{Total}	**1830.13**	**1824.32**	**2682.60**	**2635.15**	**3727.43**	**3536.79**

Table S4. Analysis of the topological properties for the free base and cationic structures of morphine and cocaine by using the hybrid B3LYP/6-31G* level of theory.

Free base/MORPHINE/Gas							
Parameter (a.u.)	**O1---H39**	**RCPN**	**RCP1**	**RCP2**	**RCP3**	**RCP4**	**RCP5**
$\rho(r_c)$	0.0218	0.0203	0.0177	0.0414	0.0181	0.0184	0.0204
$\nabla^2\rho(r_c)$	0.0814	0.1096	0.1181	0.2944	0.1188	0.1206	0.1609
λ_1	-0.0260	-0.0197	-0.0116	-0.0451	-0.0122	-0.0131	-0.0147
λ_2	-0.0178	0.0248	0.0575	0.1581	0.0615	0.0545	0.0748
λ_3	0.1252	0.1045	0.0721	0.1814	0.0695	0.0791	0.1008
$/\lambda_1/\lambda_3$	0.2077	0.1885	0.1609	0.2486	0.1755	0.1656	0.1458
Distance (Å)	2.097						
Free base/PCM							
Parameter (a.u.)	**H28---H34**	**RCPN**	**RCP1**	**RCP2**	**RCP3**	**RCP4**	**RCP5**
(r_c)	0.0107	0.0105	0.0179	0.0415	0.0181	0.0184	0.0203
$\nabla^2\rho(r_c)$	0.0438	0.0492	0.1198	0.2951	0.1178	0.1208	0.1600
$_1$	-0.0106	-0.0089	-0.0116	-0.0449	-0.0125	-0.0129	-0.0146
$_2$	-0.0043	0.0049	0.0593	0.1582	0.0598	0.0557	0.0743
$_3$	0.0586	0.0531	0.0720	0.1819	0.0704	0.0780	0.1000
$_1/_3$	0.1809	0.1676	0.1611	0.2468	0.1776	0.1654	0.1460
Distance (Å)	2.117						
Cation/ MORPHINE Gas							
Parameter (a.u.)			**RCP1**	**RCP2**	**RCP3**	**RCP4**	**RCP5**
(r_c)			0.0166	0.0434	0.0177	0.0186	0.0166
$\nabla^2\rho(r_c)$			0.1104	0.3092	0.1100	0.1207	0.1104
λ_1			-0.0119	-0.0447	-0.0123	-0.0139	-0.0119
λ_2			0.0522	0.1646	0.0598	0.0514	0.0522
λ_3			0.0700	0.1893	0.0625	0.0831	0.0700
$/\lambda_1/\lambda_3$			0.1700	0.2361	0.1968	0.1673	0.1700
Cation/PCM							
Parameter (a.u.)	**H28---H34**	**RCPN**	**RCP1**	**RCP2**	**RCP3**	**RCP4**	**RCP5**
$\rho(r_c)$	0.0104	0.0102	0.0177	0.0415	0.0179	0.0186	0.0203
$\nabla^2\rho(r_c)$	0.0434	0.0468	0.1194	0.2958	0.1117	0.1216	0.1600
λ_1	-0.0098	-0.0084	-0.0115	-0.0448	-0.0127	-0.0132	-0.0147
λ_2	-0.0036	0.0042	0.0591	0.1594	0.0597	0.0541	0.0743
λ_3	0.0569	0.0510	0.0717	0.1812	0.0647	0.0805	0.1003
$/\lambda_1/\lambda_3$	0.1722	0.1647	0.1604	0.2472	0.1963	0.1640	0.1466
Distance (Å)	2.113						
Free base/COCAINE/Gas							
Parameter (a.u.)	**O3---H31**	RCPN	RCP1	RCP2	RCP3		
$\rho(r_c)$	0.0082	0.0080	0.0202	0.0194	0.0393		
$\nabla^2\rho(r_c)$	0.0316	0.0348	0.1617	0.1252	0.2660		
λ_1	-0.0069	-0.0052	-0.0152	-0.0131	-0.0399		
λ_2	-0.0036	0.0043	0.0878	0.0595	0.1489		
λ_3	0.0422	0.0356	0.0892	0.0787	0.1569		
$/\lambda_1/\lambda_3$	0.1635	0.1461	0.1704	0.1665	0.2543		
Distance (Å)	2.627						
Free base/PCM							
Parameter (a.u.)	**O3---H31**	RCPN	RCP1	RCP2	RCP3		
$\rho(r_c)$	0.0074	0.0074	0.0201	0.0193	0.0395		
$\nabla^2\rho(r_c)$	0.0294	0.0307	0.1612	0.1236	0.2654		
λ_1	-0.0059	-0.0053	-0.0152	-0.0133	-0.0402		
λ_2	-0.0014	0.0016	0.0873	0.0587	0.1469		
λ_3	0.0367	0.0343	0.0890	0.0782	0.1586		
$/\lambda_1/\lambda_3$	0.1608	0.1545	0.1708	0.1701	0.2535		
Distance (Å)	2.690						
Cation/ COCAINE/Gas							

Parameter (a.u.)	**O3---H44**	RCPN	RCP1	RCP2	RCP3		
$\rho(r_c)$	0.0419	0.0165	0.0201	0.0188	0.0374		
$\nabla^2\rho(r_c)$	0.1304	0.0989	0.1614	0.1164	0.2535		
λ_1	-0.0645	-0.0123	-0.0152	-0.0127	-0.0372		
λ_2	-0.0631	0.0479	0.0877	0.0551	0.1442		
λ_3	0.2580	0.0632	0.0889	0.0741	0.1465		
λ_1/λ_3	0.2500	0.1946	0.1710	0.1714	0.2539		
Distance (Å)	1.778						
Cation/PCM							
Parameter (a.u.)	**O3---H44**	RCPN1	**C19---H38**	RCPN1	RCP1	RCP2	RCP3
$\rho(r_c)$	0.0298	0.0145	0.0005	0.0005	0.0201	0.0188	0.0377
$\nabla^2\rho(r_c)$	0.0894	0.0827	0.0021	0.0025	0.1612	0.1174	0.2563
λ_1	-0.0402	-0.0104	-0.0002	-0.0001	-0.0152	-0.0128	-0.0378
λ_2	-0.0388	0.0378	-0.0001	0.0002	0.0872	0.0559	0.1455
λ_3	0.1685	0.0553	0.0024	0.0024	0.0891	0.0743	0.1485
λ_1/λ_3	0.2386	0.1881	0.0833	0.0417	0.1706	0.1723	0.2545
Distance (Å)	1.942		4.038				

Table S5. Analysis of the topological properties for the hydrochloride structures of morphine and cocaine by using the hybrid B3LYP/6-31G* level of theory.

Hydrochloride/MORPHINE/GAS											
Parameter (a.u.)	**Cl42---H22**	**RCPN1**	**Cl42---H25**	**RCPN2**	**Cl42---H41**	**RCPN3**	**RCP1**	**RCP2**	**RCP3**	**RCP4**	**RCP5**
$\rho(r_c)$	0.0105	0.0098	0.0065	0.0064	0.0724	0.0098	0.0176	0.0414	0.0179	0.0186	0.0204
$\nabla^2\rho(r_c)$	0.0329	0.0380	0.0208	0.0228	0.0957	0.0380	0.1176	0.2947	0.1132	0.1212	0.1608
λ_1	-0.0085	-0.0081	-0.0040	-0.0035	-0.1168	-0.0081	-0.0116	-0.0451	-0.0126	-0.0134	-0.0147
λ_2	-0.0055	0.0058	-0.0019	0.0025	-0.1166	0.0058	0.0569	0.1595	0.0602	0.0534	0.0748
λ_3	0.0469	0.0402	0.0268	0.0238	0.3291	0.0402	0.0723	0.1803	0.0655	0.0812	0.1007
$/\lambda_1/\lambda_3$	0.1812	0.2015	0.1493	0.1471	0.3549	0.2015	0.1604	0.2501	0.1924	0.1650	0.1460
Distance (Å)	2.760		3.038		1.762						
Hydrochloride/MORPHINE/PCM											
Parameter (a.u.)	**H28---H34**	**RCPN**	**O1---H39**	**RCPN2**			**RCP1**	**RCP2**	**RCP3**	**RCP4**	**RCP5**
$\rho(r_c)$	0.0108	0.0106	0.0207	0.0198			0.0176	0.0414	0.0178	0.0185	0.0203
$\nabla^2\rho(r_c)$	0.0450	0.0490	0.0800	0.1042			0.1178	0.2948	0.1117	0.1216	0.1602
λ_1	-0.0104	-0.0086	-0.0237	-0.0187			-0.0117	-0.0449	-0.0126	-0.0132	-0.0147
λ_2	-0.0044	0.0052	-0.0143	0.0192			0.0574	0.1597	0.0591	0.0547	0.0742
λ_3	0.0596	0.0524	0.1182	0.1036			0.0720	0.1799	0.0652	0.0801	0.1007
$/\lambda_1/\lambda_3$	0.1745	0.1641	0.2005	0.1805			0.1625	0.2496	0.1933	0.1648	0.1460
Distance (Å)	2.101		2.133								
Hydrochloride/COCAINE/GAS											
Parameter (a.u.)	**O3---O1**	**RCPN1**	**Cl45---H31**	**RCPN2**	**Cl45---H37**	**RCPN3**	**Cl45---H44**	**RCPN4**	**RCP1**	**RCP2**	**RCP3**
$\rho(r_c)$	0.0143	0.0126	0.0105	0.0092	0.0083	0.0061	0.0603	0.0092	0.0202	0.0189	0.0381
$\nabla^2\rho(r_c)$	0.0501	0.0629	0.0341	0.0376	0.0276	0.0253	0.0984	0.0376	0.1617	0.1186	0.2580
λ_1	-0.0124	-0.0100	-0.0086	-0.0068	-0.0067	-0.0039	-0.0906	-0.0068	-0.0152	-0.0127	-0.0377
λ_2	-0.0109	0.0172	-0.0064	0.0080	-0.0062	0.0058	-0.0900	0.0080	0.0879	0.0553	0.1459
λ_3	0.0734	0.0557	0.0492	0.0363	0.0405	0.0234	0.2789	0.0363	0.0891	0.0759	0.1498
$/\lambda_1/\lambda_3$	0.1689	0.1795	0.1748	0.1873	0.1654	0.1667	0.3248	0.1873	0.1706	0.1673	0.2517
Distance (Å)	2.750		2.744		2.838		1.843				
Hydrochloride/ COCAINE/PCM											
Parameter (a.u.)	**O3---O1**	**RCPN1**	**Cl45---H31**	**RCPN2**	**Cl45---H37**	**RCPN3**	**Cl45---H44**	**RCPN4**	**RCP1**	**RCP2**	**RCP3**
$\rho(r_c)$	0.0141	0.0126			0.0034	0.0027	0.0369	0.0027	0.0201	0.0188	0.0380
$\nabla^2\rho(r_c)$	0.0487	0.0616			0.0100	0.0107	0.0728	0.0107	0.1612	0.1176	0.2578
λ_1	-0.0126	-0.0095			-0.0023	-0.0006	-0.0453	-0.0006	-0.0152	-0.0128	0.0375
λ_2	-0.0105	0.0164			-0.0021	0.0026	-0.0451	0.0026	0.0873	0.0545	0.1450
λ_3	0.0718	0.0548			0.0144	0.0087	0.1632	0.0087	0.0889	0.0758	0.1502
$/\lambda_1/\lambda_3$	0.1755	0.1734			0.1597	0.0690	0.2776	0.0690	0.1710	0.1689	-0.2497
Distance (Å)	2.755		3.153		3.309		2.088				

Table S6. Calculated HOMO and LUMO orbitals, energy band gap, chemical potential (μ), electronegativity (χ), global hardness (η), global softness (S), global electrophilicity index (ω) and global nucleophilicity index (E) for the free base, cationic and hydrochloride structures of morphine, cocaine and tropane by using the hybrid B3LYP/6-31G* level of theory.

MORPHINE[a]						
Frontier orbitals (eV)	Free base	Cationic	Hydrochloride			
	Gas	PCM	Gas	PCM	Gas	PCM
HOMO	-5.5670	-5.3367	-8.5413	-8.4347	-5.8917	-5.1973
LUMO	0.0374	0.1383	-3.3524	-3.4103	-0.4500	-0.6133
GAP	-5.6044	-5.4750	-5.1889	-5.0244	-5.4417	-4.5840
Descriptors (eV)						
c	-2.8022	-2.7375	-2.5945	-2.5122	-2.7209	-2.2920
m	-2.7648	-2.5992	-5.9469	-5.9225	-3.1709	-2.9053

h	2.8022	2.7375	2.5945	2.5122	2.7209	2.2920
S	0.1784	0.1826	0.1927	0.1990	0.1838	0.2182
w	1.3639	1.2339	6.8155	6.9811	1.8476	1.8414
E	-7.7475	-7.1153	-15.4288	-14.8785	-8.6274	-6.6589
COCAINE[b]						
Frontier orbitals (eV)	Free base	Cationic	Hydrochloride			
	Gas	PCM	Gas	PCM	Gas	PCM
HOMO	-5.9267	-6.0125	-9.3162	-9.2302	-5.6938	-4.9833
LUMO	-1.0687	-1.0638	-3.8694	-3.7642	-1.1856	-1.3020
GAP	-4.858	-4.9487	-5.4468	-5.4660	-4.5082	-3.6813
Descriptors (eV)						
c	-2.4290	-2.4744	-2.7234	-2.7330	-2.2541	-1.8407
m	-3.4977	-3.5382	-6.5928	-6.4972	-3.4397	-3.1427
h	2.4290	2.4744	2.7234	2.7330	2.2541	1.8407
S	0.2058	0.2021	0.1836	0.1829	0.2218	0.2716
w	2.5183	2.5297	7.9799	7.7229	2.6244	2.6828
E	-8.4959	-8.7546	-17.9548	-17.7568	-7.7534	-5.7845
TROPANE ALKALOID[c]						
Frontier orbitals (eV)	Free base	Cationic	Hydrochloride			
	Gas	PCM	Gas	PCM	Gas	PCM
HOMO	-5.4945	-5.6725	-12.9365	-12.9433	-5.5910	-4.9043
LUMO	2.0561	1.9886	-3.3770	-3.4183	1.2336	1.0076
GAP	-7.5506	-7.6611	-9.5595	-9.5250	-6.8246	-5.9119
Descriptors (eV)						
c	-3.7753	-3.8306	-4.7798	-4.7625	-3.4123	-2.9560
m	-1.7192	-1.8420	-8.1567	-8.1808	-2.1787	-1.9483
h	3.7753	3.8306	4.7798	4.7625	3.4123	2.9560
S	0.1324	0.1305	0.1046	0.1050	0.1465	0.1691
w	0.3914	0.4429	6.9598	7.0263	0.6955	0.6421
E	-6.4905	-7.0557	-38.9872	-38.9613	-7.4343	-5.7592

χ = - [E(LUMO) - E(HOMO)]/2; μ = [E(LUMO) + E(HOMO)]/2; η = [E(LUMO) – E(HOMO)]/2;
$S = \frac{1}{2}h$; $w = m^2/2h$; $E = m*h$
[a]This work, [b]From Ref [30], [c]From Ref [31]

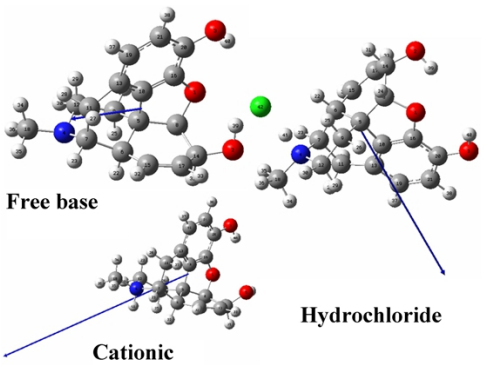

Figure S1. Dipole moment values for the free base, cationic and hydrochloride morphine species calculated in gas phase at the B3LYP/6-31G* level of theory showing the corresponding magnitudes and orientations of their vectors.

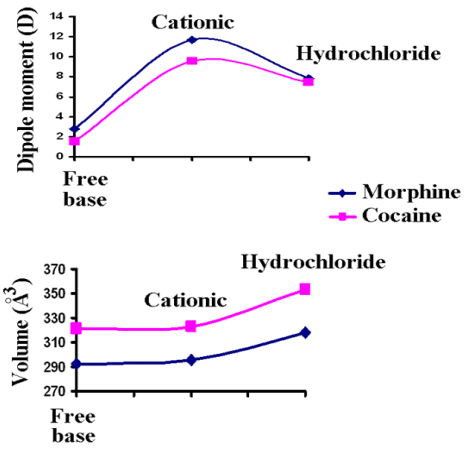

Figure S2. Dipole moment and volume variations for the free base, cationic and hydrochloride morphine species calculated in gas phase at the B3LYP/6-31G* level of theory compared with those corresponding to the three cocaine species [31].

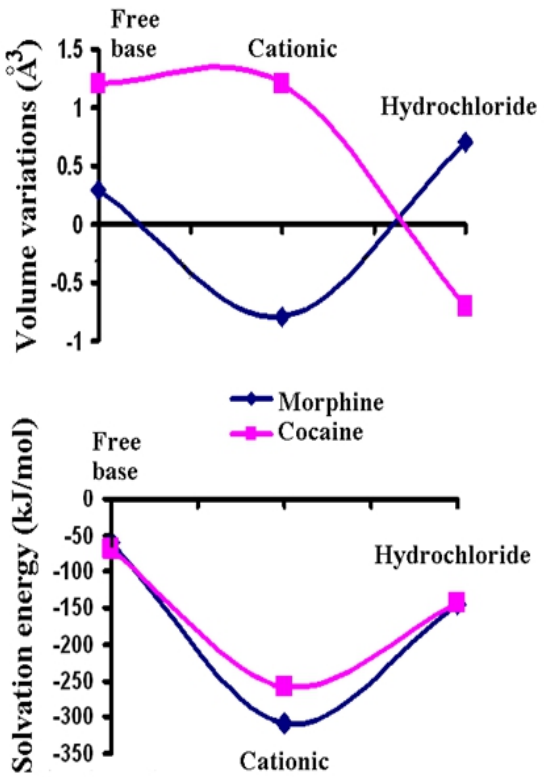

Figure S3. Volume and solvation energy variations for the free base, cationic and hydrochloride morphine species calculated in gas phase at the B3LYP/6-31G* level of theory compared with those corresponding to the three cocaine species [31].

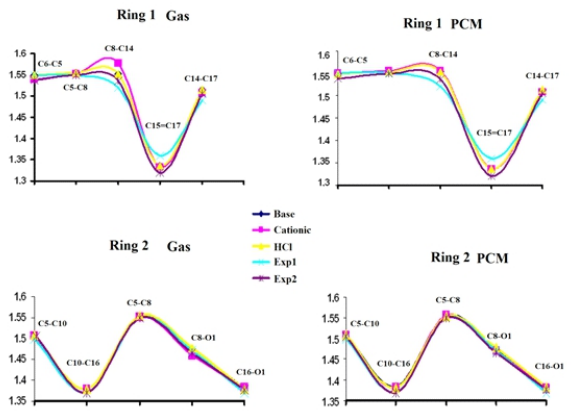

Figure S4. Theoretical geometrical parameters obtained for the bonds that belong to the R1 (top) and R2 Rings (bottom) of the three morphine species calculated in gas phase and aqueous solution at the B3LYP/6-31G* level of theory compared with those experimental corresponding to hydrochloride morphine [22].

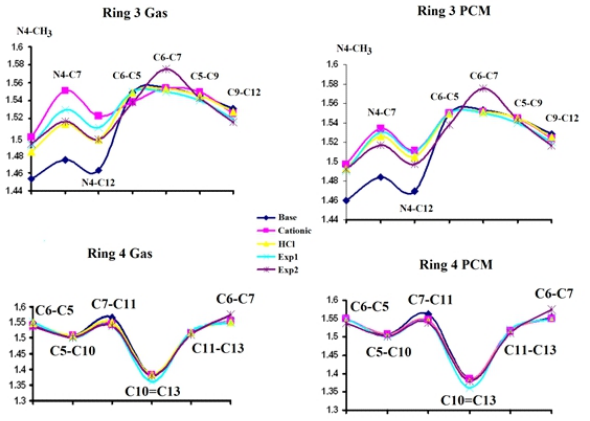

Figure S5. Theoretical geometrical parameters obtained for the bonds that belong to the R3 (top) and R4 (bottom) rings of the three morphine species calculated in gas phase and aqueous solution at the B3LYP/6-31G* level of theory compared with those experimental corresponding to hydrochloride morphine [22].

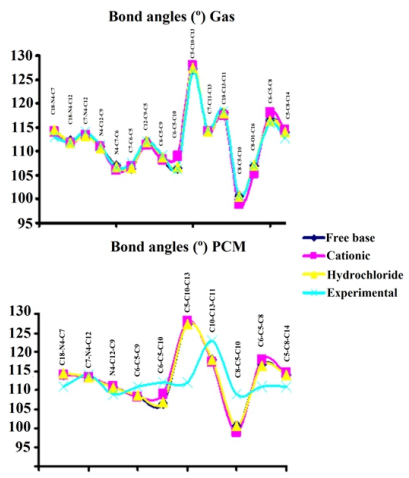

Figure S6. Theoretical bond angles of the three morphine species calculated in gas phase (top) and aqueous solution (bottom) at the B3LYP/6-31G* level of theory compared with those experimental corresponding to hydrochloride morphine [22].

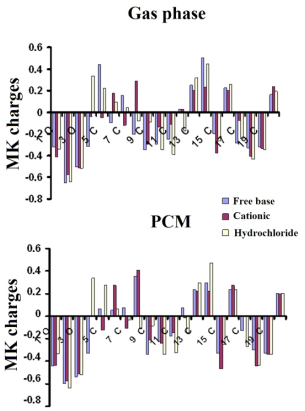

Figure S7. Variations of the MK charges on the O, N and C atoms corresponding to the free base, cationic and hydrochloride morphine species calculated in gas phase (upper) and aqueous solution (bottom) at the B3LYP/6-31G* level of theory.

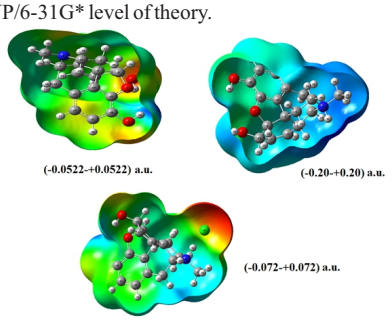

Figure S8. Calculated electrostatic potential surfaces on the molecular surfaces of the free base, cationic and hydrochloride morphine species in gas phase. Color ranges. In au: from red -0.056 to blue +0.056. B3LYP functional and 6-31G* basis set. Isodensity value of 0.005.

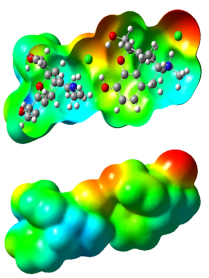

Figure S9. Calculated electrostatic potential surfaces on the molecular surfaces of the hydrochloride dimer species in gas phase. Color ranges. In au: from red -0.056 to blue +0.056. B3LYP functional and 6-31G* basis set. Isodensity value of 0.005.

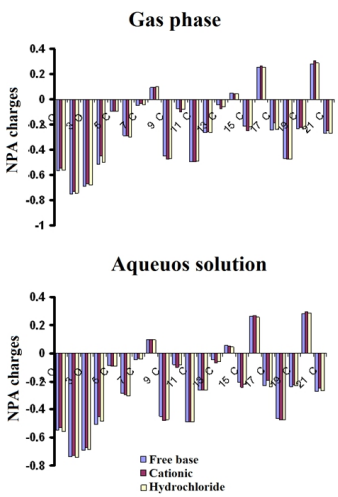

Figure S10. Variations of the bond orders for all C atoms corresponding to the five rings of the free base, cationic and hydrochloride cocaine species calculated in gas phase at the B3LYP/6-31G* level of theory.

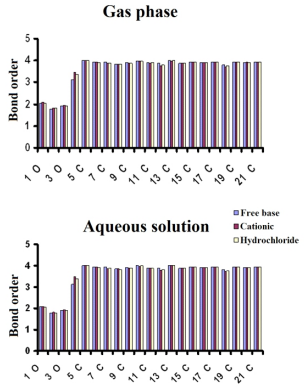

Figure S11. Variations of the bond orders for the C atoms corresponding to the pyrrolidine (C6, C7, C9 and C10) and piperidine (C6, C7, C8, C11 and C12) rings of the free base, cationic and hydrochloride cocaine species calculated in gas phase at the B3LYP/6-31G* level of theory.

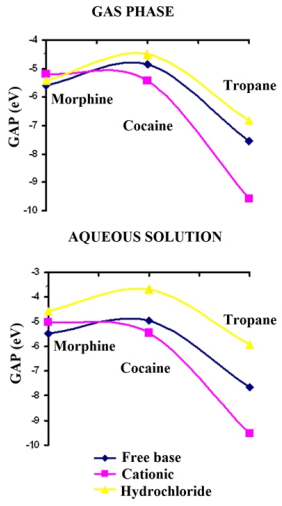

Figure S12. Gap values for the free base, cationic and hydrochloride species of morphine, cocaine and tropane alkaloids in gas (Top) and aqueous solution (Bottom) phases at the B3LYP/6-31G* level of theory.

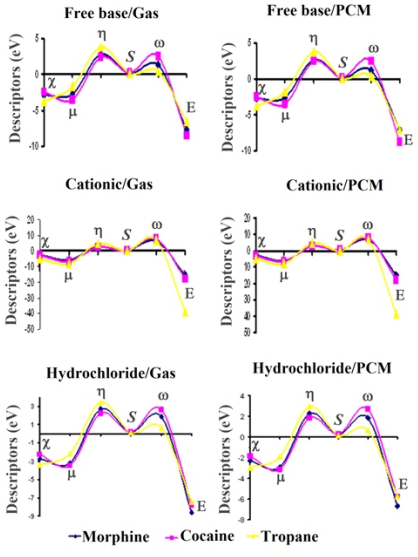

Figure S13. Descriptors calculated for the free base, cationic and hydrochloride cocaine species in gas and aqueous solution phases at the B3LYP/6-31G* level of theory.

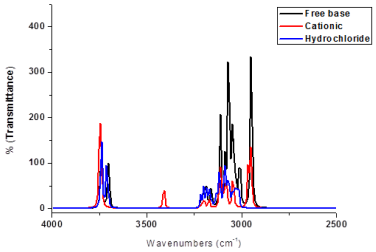

Figure S14. Theoretical infrared spectra for the free base, cationic and hydrochloride morphine species in gas phase in the 4000-2500 cm-1 region at the B3LYP/6-31G* level of theory.

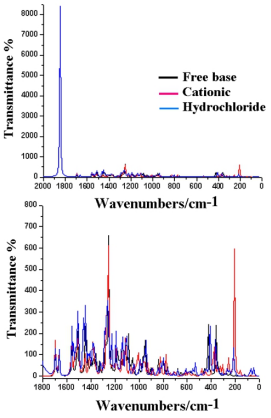

Figure S15. Theoretical infrared spectra for the free base, cationic and hydrochloride morphine species in gas phase in the 2000-0 cm^{-1} (upper) and 1800-0 cm-1 (bottom) regions at the B3LYP/6-31G* level of theory.

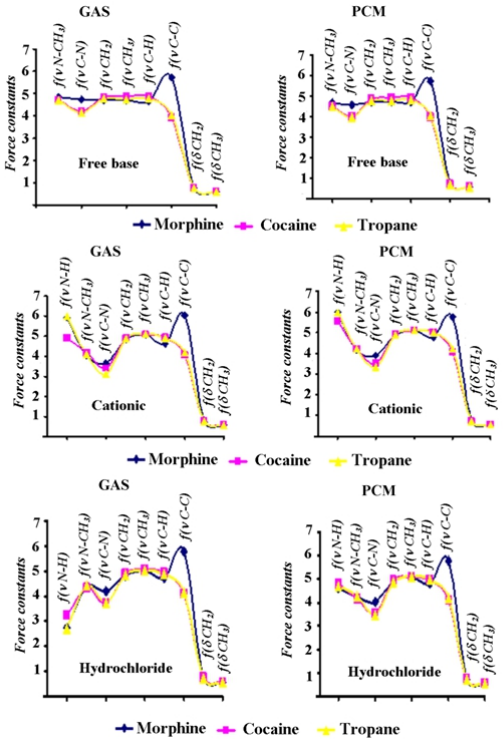

Figure S16. Force constants calculated for the free base, cationic and hydrochloride morphine species compared with those calculated for the corresponding species of cocaine and tropane alkaloids in gas and aqueous solution phases at the B3LYP/6-31G* level of theory.

REFERENCES:

[1] Gates, M.; Tschudi, G. (1952), The synthesis of morphine, J. Amer. Chem. Soc. 74, 1109-1110.
[2] Gates, M.; Tschudi, G. (1956), The synthesis of morphine. J Am Chem Soc. 78, 1380–1393
[3] Reed, J.W.; Hudlicky, T. (2015), The Quest for a Practical Synthesis of Morphine Alkaloids and Their Derivatives by Chemoenzymatic Methods, Acc. Chem. Res. 48(3), 674–687.
[4] Rinner, U.; Hudlicky, T. (2012), Synthesis of Morphine Alkaloids and Derivatives, Top Curr Chem 309, 33–66.
[5] Galanie, S.; Thodey, K.; Trenchard, I.J.; Filsinger Interrante, M.; Smolke, C.D. (2015), Complete biosynthesis of opioids in yeast, Science express, 1-11, 10.1126/science.aac 9373.
[6] Galanie, S.; Thodey, K.; Trenchard, I.J.; Filsinger Interrante, M.; Smolke, C.D. (2015), Complete biosynthesis of opioids in yeast, Science, 349(6252), 1095–1100.
[7] Busse, G.D. DRUGS, The Straight Facts, Morphine, Consulting Editor David J. Triggle, Chelsea House Publishers, New Cork (2006).
[8] Buckett, W.R; Haining, C.G. (1965), Some pharmacological studies on the optically active isomers of hyoscine and hyoscyamine, Brit. J. Pharmacol. 24, 138-146.
[9] Cantor, E.; Abraham, S.; Marcum, E.A.; Spector, S. 90 (1983), Structure-activity requirements for hypotension and et-adrenergic receptor blockade by analogues of atropine, European Journal of Pharmacology, 75-83.
[10] Hammon, K.; De Martino, B. (1985), Postoperative Delirium Secondary to Atropine Premedication, Anesthesia Progress 107-108.
[11] Armstrong, D.W.; Han, S.M.; Han, Y.I. (1987), Separation of Optical Isomers of Scopolamine, Cocaine, Homatropine, and Atropine, Analytical Biochemistry 167, 261-264.
[12] Niu, Y-Y; Yang, L-M; Liu, H-Z; Cui, Y-Y; Zhu, L.; Feng, J-M; Yao, J-H; Chen, H-Z; Fan, B-T; Chen, Z-N; Lu, Y. (2005), Activity and QSAR study of baogongteng A and its derivatives as muscarinic agonists, Bioorganic & Medicinal Chemistry Letters 15, 4814–4818.
[13] Xiang, X-H; Wang, H-L; Wu, W-R; Guo, Y.; Cao, D-Y; Wang, H-S; Zhao, Y; (2006), Ethological analysis of scopolamine treatment or pretreatment in morphine dependent rats, Physiology & Behavior 88, 183–190.
[14] De Simone, R.; Margarucci, L.; De Feo, V. (2008), Tropane alkaloids: An overview, Pharmacologyonline, 170-89.
[15] Beyer, J.; Drummer, O.H.; Maurer, H.H. (2009), Analysis of toxic alkaloids in body samples, Forensic Science International 185, 1–9.
[16] Klinkenberg, I.; Blokland, (2010), A. The validity of scopolamine as a pharmacological model for cognitive impairment: A review of animal behavioral studies, Neuroscience and Biobehavioral Reviews 34, 1307–1350.
[17] Wang, J-H.; Chena, Y-M.; Carlson, S.; Li, L.; Hu, X-T.; Ma, Y-Y. (2012), Interactive effects of morphine and scopolamine, MK-801, propanolol on spatial working memory in rhesus monkeys, Neuroscience Letters 523, 119– 124.
[18] Veeranjaneyulu, P.; Rao, T.B.; Mantha, S.; Vaidyanathan, G. (2012), A sensitive method for the estimation of scopolamine um human plasma using ACQUITY UPLC and Xevo TQ-S, Waters Corporation, Bangalore, India, 1-7.
[19] Sweta, V.R.; Lakshmi, T. (2015), Pharmacological profile of tropane alkaloids, Journal of Chemical and Pharmaceutical Research, 7(5), 117-119.
[20] Gylbert, L. (1973), The Crystal and Molecular Structure of Morphine Hydrochloride Trihydrate, Acta Cryst B29, 1630.
[21] Gelbrich, T.; Braun, D.E.; Griesser, U.J. (2012), Morphine hydrochloride anhydrate, Acta Cryst. E68, o3358–o3359.
[22] Gelbrich, T.; Braun, D.E.; Griesser, U.J. (2013), Stable polymorph of morphine, Acta Cryst. E69, o2.
[23] Pandey, A.K.; Dwivedi, A.; Siddiqui, S.A.; Misra, N. (2013), Vibrational Spectra of Two Narcotics. A DFT Study, Chinese J. of Physics 51(3), 473-499.
[24] Baranska, M.; Kaczor, A. (2012), Morphine studied by vibrational spectroscopy and DFT calculations, J. Raman Spectrosc. 43, 102–107.
[25] Lazny, R.; Ratkiewicz, A.; Nodzewska, A.; Wynimko, A.; Siergiejczyk, L. (2012), Determination of the N-methyl stereochemistry in tropane and granatane derivatives in solution: a computational and NMR spectroscopic study, Tetrahedron Letters.
[26] Becke, A.D. (1988), Density-functional exchange-energy approximation with correct asymptotic behavior, Phys. Rev., A38, 3098-3100.
[27] Lee, C.; Yang, W.; Parr. R.G. (1995), Development of the Colle-Salvetti correlation-energy formula into a functional of the electron density, Phys. Rev. B37 (1988) 785-789.
[28] a) Rauhut, G.; Pulay, (1995), P. J. Phys. Chem. 99, 3093-3099. b) Correction: Rauhut, G.; Pulay, P. J (1995), Phys. Chem. 99, 14572.
[29] Sundius, T. (2002), Scaling of ab initio force fields by MOLVIB, Vib. Spectrosc. 29, 89-95.
[30] Rudyk, R.; Brandán, S.A. (2017), Vibrational assignment of alkaloid tropane hydrochloride by using their infrared spectrum, internal coordinates and the SQM procedure, submitted to Comp. Theor. Chem..
[31] Romani, D.; Brandán, S.A. (2017), Vibrational analyses of alkaloid cocaine as free base, cationic and hydrochloride species based on their internal coordinates and force fields, submitted to Comp. Theor. Chem..
[32] Parr, R.G.; Pearson, R.G. (1983), Absolute hardness: companion parameter to absolute electronegativity, J. Am. Chem. Soc. 105, 7512-7516.
[33] Brédas, J-L (2014), Mind the gap!, Materials Horizons 1, 17–19.
[34] Romani, D.; Márquez, M.J.; Márquez, M.B.; Brandán, S.A. (2015), Structural, topological and vibrational properties of an isothiazole derivatives series with antiviral activities, J. Mol. Struct. 1100, 279-289.
[35] Romani, D.; Tsuchiya, S.; Yotsu-Yamashita, M.; Brandán, S.A. (2016), Spectroscopic and structural investigation on intermediates species structurally associated to the tricyclic bisguanidine compound and to the toxic agent, saxitoxin, J. Mol. Struct. 1119, 25-38.
[36] Chain, F.; Iramain, M.A; Grau, A.; Catalán, C.A.N.; Brandán, S.A. (2016), Evaluation of the structural, electronic, topological and vibrational properties of N-(3,4-dimethoxybenzyl)-hexadecanamide isolated from Maca (Lepidium meyenii) using different spectroscopic techniques, J. Mol. Struct. 1119, 25-38.
[37] Issaoui, N.; Ghalla, H.; Brandán, S.A.; Bardak, F.; Flakus, H.T.; Atac, A.; Oujia, B. (2017), Experimental FTIR and FT-Raman and theoretical studies on the molecular structures of monomer and dimer of 3-thiopheneacrylic acid, J. Mol. Structure 1135, 209-221.
[38] Nielsen, A.B.; Holder, A.J. Gauss View 3.0, User's Reference, GAUSSIAN Inc., Pittsburgh, PA, 2000–2003.
[39] Frisch MJ, Trucks GW, Schlegel HB, Scuseria GE, Robb MA, Cheeseman JR, et al. Gaussian 09, Revision D.01, Gaussian, Inc., Wallingford CT, 2009.
[40] Miertus, S.; Scrocco, E.; Tomasi, J. (1981), Electrostatic interaction of a solute with a continuum. Chem. Phys. 55, 117–129.
[41] Tomasi, J.; Persico, J. (1994), Molecular Interactions in Solution: An Overview of Methods Based on Continous Distributions of the Solvent, Chem. Rev. 94, 2027-2094.
[42] Marenich, A.V.; Cramer, C.J.; Truhlar, D.G. (2009) Universal solvation model based on solute electron density and a continuum model of the solvent defined by the bulk dielectric constant and atomic surface tensions, J. Phys. Chem. B113, 6378-6396.
[43] Ugliengo, P., Moldraw Program, University of Torino, Dipartimento Chimica IFM, Torino, Italy, 1998.
[44] Glendening, E.D.; Badenhoop, J.K.; Reed, A.D.; Carpenter, J. E.; Weinhold, F. NBO 3.1; Theoretical Chemistry Institute, University of Wisconsin; Madison, WI, 1996.
[45] Besler, B.H.; Merz Jr, K.M.; Kollman, P.A. (1990), Atomic charges derived from demiempirical methods, J. Comp. Chem. 11, 431-439.
[46] Biegler-Kŏning, F.; Schönbohm, J.; Bayles, D. (2001), AIM2000; A Program to Analyze and Visualize Atoms in Molecules, J. Comput. Chem. 22, 545.
[47] Bader, R.F.W. Atoms in Molecules, A Quantum Theory, Oxford University Press, Oxford, 1990, ISBN: 0198558651.
[48] Infrared spectrum Morphine, NIST Chemistry WedBook (http://webook.nist.gov/chemistry).
[49] Keresztury, G.; Holly, S.; Besenyei, G.; Varga, J.; Wang, A.Y.; Durig, J.R. (1993), Vibrational spectra of monothiocarbamates-II. IR and Raman spectra, vibrational assignment, conformational analysis and ab initio calculations of S-methyl-N,N-dimethylthiocarbamate Spectrochim. Acta, 49A, 2007-2026.
[50] Michalska, D.; Wysokinski, R. (2005), The prediction of Raman spectra of platinum(II) anticancer drugs by density functional theory, Chemical Physics Letters, 403, 211-217.
[51] Romano, E.; Davies, L.; Brandán, S.A. (2017), Structural properties and FTIR-Raman spectra of the anti-hypertensive clonidine hydrochloride agent and their dimeric species, J. Mol. Struct. 1133, 226-235.
[52] Márquez, M.B.; Brandán, S.A. (2014), A Structural and Vibrational Investigation on the Antiviral Deoxyribonucleoside Thymidine Agent in Gas and Aqueous Solution Phases, Int. J. Quantum Chem. 114, 209-221.
[53] Cataldo, P.G.; Castillo, M.V.; Brandán, S.A. (2014), Quantum Mechanical Modeling of Fluoromethylated-pyrrol Derivatives a Study on their Reactivities, Structures and Vibrational Properties, J Phys Chem Biophys, 4(1), 4-9.
[54] Márquez, M.J.; Márquez, M.B.; Cataldo, P.G.; Brandán, S.A. (2015), A Comparative Study on the Structural and Vibrational Properties of Two Potential Antimicrobial and Anticancer Cyanopyridine Derivatives, Open Journal of Synthesis Theory and Applications, 4, 1-19.